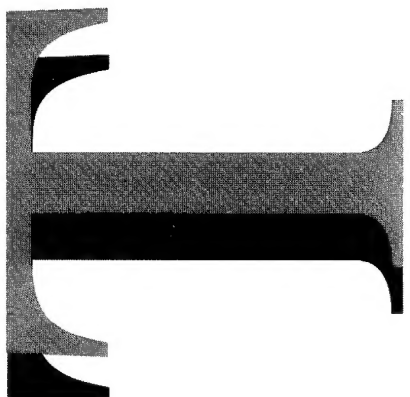


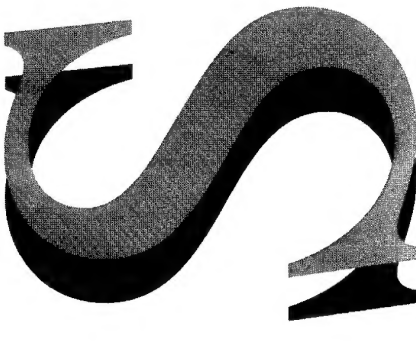
AR-008-405

DSTO-TR-0229



Investigation of Fatigue Cracking
on LAU-7/A Launcher Housing

D.S. Saunders, M.G. Stimson,
R. Bailey and E. Kowal



DISTRIBUTION STATEMENT A
Approved for public release

APPROVED FOR PUBLIC RELEASE

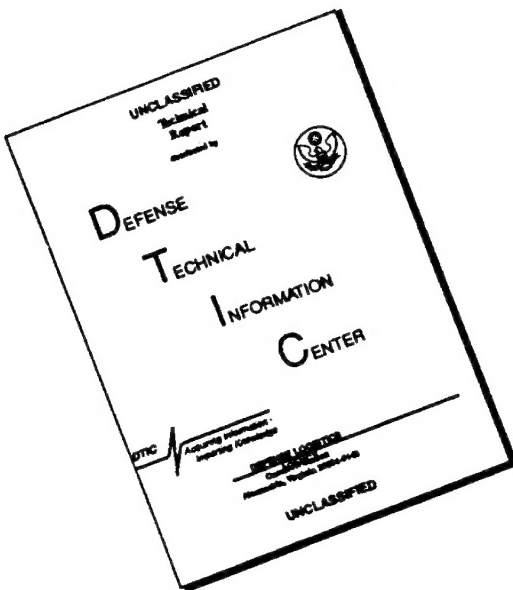
(C) Commonwealth of Australia

19961009 141



DEPARTMENT OF DEFENCE
DEFENCE SCIENCE AND TECHNOLOGY ORGANISATION

DISCLAIMER NOTICE



**THIS DOCUMENT IS BEST
QUALITY AVAILABLE. THE COPY
FURNISHED TO DTIC CONTAINED
A SIGNIFICANT NUMBER OF
PAGES WHICH DO NOT
REPRODUCE LEGIBLY.**

Investigation of Fatigue Cracking on LAU-7/A Launcher Housing

D.S. Saunders, M.G. Stimson, R. Bailey and E. Kowal

**Airframes and Engines Division
Aeronautical and Maritime Research Laboratory**

DSTO-TR-0229

ABSTRACT

A number of LAU-7/A launcher housings on Australian F/A-18 aircraft have been found to be fatigue cracked at the location of the forward missile hanging bracket. This was initially ascribed to poor aft snubbing of the missile in the launcher guide rail.

An investigation of the response of the LAU-7/A launcher housing configuration to static and fatigue loading was undertaken to determine the failure mechanism.

A test fixture was designed to apply static loads to a launcher housing via a dummy AIM-9 missile. The results showed that the strains at the points of engagement of the missile hanging brackets with the launcher guide rail were not significantly influenced by the effectiveness of the aft snubbing of the missile.

The launcher housing was then fatigue tested using spectrum loading. The loads applied to the test articles were derived from a number of N_Z load spectra of Australian F/A-18 aircraft. The load levels were factored up to account for the dynamic effects of the flexible wings of the aircraft. To ascertain whether the loads achieved in the experimental study were appropriate for the fatigue testing of the component, the fracture surfaces derived from the fatigue test were compared with several surfaces removed from launcher housings which had failed under operational loads. The results showed that the use of "factored" N_Z loads was only an approximate simulation of the wing tip environment, but in the absence of a wing tip spectrum these loads gave approximately similar fatigue fracture surfaces to those of the components in service.

The results showed that the cracking was largely induced by the inertial loads experienced by the missile, which are transferred to the guide rails of the LAU-7/A housing.

RELEASE LIMITATION

Approved for public release

DTIC QUALITY INSPECTED 2

DEPARTMENT OF DEFENCE

DEFENCE SCIENCE AND TECHNOLOGY ORGANISATION

Published by

*DSTO Aeronautical and Maritime Research Laboratory
PO Box 4331
Melbourne Victoria 3001*

*Telephone: (03) 9626 8111
Fax: (03) 9626 8999
© Commonwealth of Australia 1995
AR No. AR-008-405
September 1995*

APPROVED FOR PUBLIC RELEASE

Investigation of Fatigue Cracking on LAU-7/A Launcher Housing

Executive Summary (U)

The LAU-7/A launcher housing is the aluminium body of the missile launcher carried on the wing tip of each F/A-18 in order to carry the AIM-9 Sidewinder Air-to-Air missile. A launcher must be carried on every flight as the component mass is necessary for the flutter protection of the aircraft wing. Three steel lugs on the missile are held into the launcher rails, along which the missile slides to clear the aircraft during firing. For normal air combat training sorties the launcher carries the externally identical Dummy Air Training Missile (DATM) which is not capable of firing and carries no warhead.

An unusually high number of cracks were found during the 3 years up to 1990. All were of launchers that had seen only hundreds of hours service and these failures were considered premature. Some were detected as structural failures by the pilots during pre-flight walk around and others by the NDI techniques during the course of normal maintenance of the launchers. All involved fatigue cracking of the guide rail near the forward of the three hanging brackets.

At the rate of cracking evident at that time, the current stocks of launchers would have lasted only a relatively short time. Supplies of replacements were uncertain, putting the operational ability of the tactical fighter fleet into question in the coming years.

In the absence of flight test loads data, AMRL was tasked with determining the cause of cracking and identifying a conceptual economic repair scheme. The investigation part of this task is reported in this work. A repair was developed at AMRL and a fatigue test and some preliminary field fatigue trials were conducted. However, after some years, replacement suppliers were located by the RAAF and the trials discontinued. In addition, a reduction in the rate of crack detection after 1991 has benefitted the launcher fleet serviceability, and this may have been due to a reduction in the occurrences of high normal accelerations in the F/A-18 fleet spectra after that time.

The investigation involved static strain surveys and a number of fatigue tests to determine the load levels which would result in the cracking seen in service. The numerous strain surveys eliminated several theories as to sources of extreme load on the forward hanger area, leaving the conclusion that the manner in which the inertia loads on the missile were transferred to the launcher was largely unaffected by service installation procedures. The fatigue test programme confirmed that, for inertial loads only, the accelerations of the missile necessary for cracking at the rate observed were in excess of 2.5 times those measured in the vertical direction at the aircraft centre-of-gravity.

The cause of cracking was thus narrowed to the highly damaging spectrum of inertia and/or aerodynamic loads being applied by the relatively severe usage of the F/A-18 prior to 1990. More definitive acceleration or loads spectra would be required to further refine the assessment of the cause of cracking. If the requirement had continued for a full flight qualification of a repair scheme, the fatigue test program to date would have provided an adequate baseline from which to confirm the improved fatigue life.

A useful result of the investigation was the development of a much improved ultrasonic technique which has become standard maintenance practice with the RAAF. The incidence of spurious crack indications has been considerably reduced, increasing the pool of serviceable launchers and saving significant replacement costs.

Authors

D.S. Saunders

Ship Structures and Materials Division

Dr. David Saunders is a Principal Research Scientist in the Ship Structures and Materials Division at AMRL. He received a B. Appl. Sc. (Hons) from Adelaide University and a Ph.D. from Monash University. He has worked for the Defence Science and Technology Organisation since 1976 and has been involved in research into the fatigue and fracture behaviour of steels, aluminium alloys and fibre reinforced composite materials for a wide range of defence applications including munitions, ordnance and air and sea platforms. Recent research has involved studies of the effects of load sequences and environment on the fatigue behaviour of thick, impact-damaged graphite/epoxy composite panels. Dr. Saunders presently manages a Task which studies the response of naval platforms and structures to underwater explosions. Dr. Saunders is a member of the Institution of Engineers, Australia and is a member of the Military Engineering and Composite Structures Societies of the IEAust.

M.G. Stimson

Airframes and Engines Division

Mr. Stimson graduated from the University of N.S.W., Sydney, in 1985, with a Bachelor of Engineering (Aeronautical) degree with honours. Since then he has contributed to various structural integrity programmes at what is now AMRL. He was posted to Northrop Aircraft Division, El Segundo, Los Angeles for all of 1990, working with the stress analysis techniques used in the design of the F/A-18. Since 1991 he has contributed to several investigations of accidents and incidents involving RAAF aircraft. He has more recently also contributed to the F/A-18 and PC-9/A flight loads test programmes conducted at RAAF Edinburgh. Mr. Stimson is currently a member of the Royal Aeronautical Society, Australian Division and the Australian Meteorological and Oceanographic Society, as well as a keen soaring pilot, instructor and airworthiness inspector.

R. Bailey
Airframes and Engines Division

For over 20 years Mr. Bailey has worked as a technical officer at AMRL constructing and running static and fatigue tests on various aircraft structures. The full-scale aircraft or major component tests he has contributed to include the fatigue tests for the Mirage 3O, CT-4A, F/A-18 Bulkheads, P3-C Orion wing leading edge, F-111C wing carry-through box, to name a few. Mr. Bailey has also participated in numerous developmental or research oriented experiments in the aircraft structural mechanics field. His recent experience also includes work laying-up composite panels for research projects in this area.

E. Kowal
Airframes and Engines Division

Miss Kowal graduated from the University of Newcastle-upon-Tyne (UK) in 1972 with a B.Sc. degree (joint honours in Botany and Genetics). In 1988 she obtained a B.App.Sc. in Scientific Photography from RMIT, Melbourne. During 1973-1977 she was involved in microscopy and botanical anatomy at the University of N.S.W., Sydney. She then worked for the NSW Department of Agriculture during 1977-1980 , involved in identifying anatomical features of merino sheep which confer resistance to fleece rot and blowfly strike. During 1980-1988 she was employed as the Divisional Photographer at CSIRO, Division of Mineral Products, Melbourne. Since 1988 she has worked at AMRL, involved in; fractography; the development of a microgridding technique to measure low strains; and its application to the study of fatigue of materials and associated components.

Contents

LIST OF TABLESiii
LIST OF FIGURES.....	v
1. INTRODUCTION.....	1
2. OBJECTIVES	4
3. EXPERIMENTAL METHODS.....	5
3.1 Fractography of LAU-7/A Launcher Housings.....	5
3.2 Static Strain Surveys.....	5
3.3 Fatigue Test of LAU-7/A Launcher Guide Rails	6
3.3.1 Preliminary Fatigue Test of Launcher 0148 (RH Rail).....	7
3.3.2 Fatigue Test of Launcher 71032-012 (LH Rail).....	8
3.3.3 Fatigue Test of Launcher 0715 (LH Rail).	8
3.3.4 Fatigue Test of Launcher 71032-012 (RH Rail)	8
3.4 Wear at Hanging Bracket Locations	8
3.5 Additional Failures.....	8
3.6 Non-Destructive Inspection of Launcher Guide Rails.....	9
4. RESULTS	9
4.1 Fractography of LAU-7/A Launcher Housings.....	9
4.1.1 Service Failures.....	9
4.1.2 Test Failures.....	10
4.2 Static Strain Surveys.....	10
4.3 Fatigue Behaviour of LAU-7/A Launcher Guide Rails	13
4.3.1 Preliminary Fatigue Test of Launcher 0148 (RH Rail).....	13
4.3.2 Fatigue Test of Launcher 71032-012 (LH Rail).....	14
4.3.3 Fatigue Test of Launcher 0715 (LH Rail)	14
4.3.4 Fatigue Test of Launcher 71023-012 (RH Rail)	14
4.4 Movement and Wear at Hanging Bracket Locations.....	14
4.5 Additional Failures.....	14
4.6 Non-Destructive Inspection of Launcher Guide Rails.....	15
5. DISCUSSION	15
5.1 Static Strain Surveys.....	15
5.2 Movement and Wear at the Hanging Bracket Locations.....	16
5.3 Fatigue Crack Growth.....	17
5.4 Fatigue Behaviour of the Launchers.....	17
5.5 Additional Failures.....	18
5.6 NDI Methodologies.....	18

6. CONCLUSIONS.....	19
7. RECOMMENDATIONS.....	19
8. ACKNOWLEDGEMENTS	20
9. REFERENCES	20
APPENDIX A LOADING EVALUATION AND FATIGUE TEST SPECTRUM DEVELOPMENT.....	45
A1. CHOICE OF SPECTRUM.....	45
A1.1 Inertial Manoeuvre Loads	45
A1.2 Aerodynamic Manoeuvre Loads	45
A1.3 Wing Vibration Loads	46
A1.4 Gust Aerodynamic Loads.	47
A1.5 Dynamic Manoeuvre Transient Loads.....	47
A1.6 Summary.....	47
A2. FATIGUE TEST SPECTRUM DEVELOPMENT	48
A2.1 Factoring of N_z Loads.	49
A3. REFERENCES	50
APPENDIX B. NDI OF LAU7/A LAUNCHER GUIDE RAILS.....	55
B1. COMPARISON OF INSPECTION TECHNIQUES.....	55
B2. SUMMARY OF AMRL ULTRASONIC METHOD, [3].	55
B2.1 Equipment:.....	55
B2.2 Set-up Procedure:.....	56
B2.3 Method of Operation	56
B3. REFERENCES.....	57

List of Tables

Table 1. Fatigue Failures of LAU-7/A Launcher Guide Rails	23
Table 2. Fatigue Crack Growth in LAU-7/A Launcher Guide Rails	23
Table 3. Crack Indications In Lau-7/A Launchers ¹ Inspected At Amrl	23
Table 4. Summary Of Static Loading Experiments on LAU-7/A Launcher Housing S/N 0230 (Worn And New Aft Snubber Kits)	24
Table 5. Comparison Of Strain Levels In The Uncracked LAU-7/A Launcher Guide Rail	25
Table 6. Displacement Of The AIM-9 Missile Forward Hanging Bracket Relative To The LAU-7/A Launcher Housing	26
Table 7. Effect On Fwd Hanger Strains Of The Stainless Steel Wear Plate Modification To Aft Snubbers ¹ Of LAU-7/A Launcher Number Nmh230	26
Table 8. Strain Response To Missile Torque Load At The Forward Hanger For Normal Snubbing And With Raaf Wear Plate	27
Table 9. Effect On The Strains At The Forward Hanger Of The Canadian Forces Teflon Cylinders As Additional Snubbers.....	27
Table A1.1. LAU-7/A Launcher Accelerometer Peak g Data (from Ref. [2]) During Typical Prescribed Manoeuvres	51
Table A1.2. AIM-9 Captive Carriage Translational and Rotational Peak Accelerations. (from Ref. [5])	52
Table A1.3. Reactions at Hangers for Captive Carriage Load Cases (Limit Loads). (from Ref. [5])	53
Table A2.1. Correspondence between LAUSEQ and Flight loads.	53
Table B1.1. Crack length measurements on LAU-7/A launcher guide rails.....	57

List of Figures

Figure 1. The wing-tip position of the LAU-7/A launcher and AIM-9 missile	28
Figure 2. Section through the LAU-7/A launcher guide rail and AIM-9 missile at the location of the forward missile hanging bracket.....	28
Figure 3. Forward snubber region with forward to the left. The snubber plates (arrowed) are in the engaged position. The hold-back detent mechanism and striker points are visible in the centre.....	29
Figure 4. The location of cracking in the LAU-7/A launcher guide rail and typical fatigue crack (inset).	29
Figure 5. Optical micrograph of the region of cracking in the guide rail of LAU-7/A launcher number 0159, from [2]. 6X.....	30
Figure 6. Scanning electron micrograph of the fracture surface from the guide rail of LAU-7/A launcher number 0159, after [2]. 16X.....	30
Figure 7. Worn scissor blades from the aft snubber mechanism. Scissors were painted black prior to cycling to illustrate the wear which reduces snubbing effectiveness	31
Figure 8. Wear of the inner corners of the aft hanging bracket corresponding to that of the scissors.	31
Figure 9. Wear of the inside surface of the rail over the contact zone of the forward hanging bracket. The hills and depressions of the wear marks cause great difficulty for NDI processes. The fatigue crack grown under the test load spectrum is difficult to discern from the overload failure zone.	32
Figure 10. The RAAF wear plate installed under the aft snubbing mechanism in an attempt to force the missile hanger against the rail and restrict vertical movement.	32
Figure 11. A cross section of the launcher-missile combination showing the CF design of teflon cylinders to increase snubbing forces. The teflon prevents damage to either part, but soon deforms and loses effectiveness.....	33
Figure 12. Launcher strain gauge positions	34
Figure 13. Front view of the test rig with an AIM-9 Sidewinder installed. The hydraulic actuator is connected to the hand pump and pressure gauge as for the static strain surveys.	35
Figure 14. Rear view of the dummy missile and launcher in the rig with the torque strap and dead weight carry attached to the rear fins.	35
Figure 15. Effect of shimming forward hanging bracket in the guide rails during a fatigue test.	36
Figure 16. Fatigue crack growth in the guide rail of launcher NMH 0217 due to service loads. Within the striation bands growth occurs at an average of 900 striations per mm.....	37

Figure 17. Another example, from a launcher found overloaded in operational service, of fatigue crack growth interspersed with ductile tearing . This scanning electron micrograph is of launcher S/N 0355.	38
Figure 18. Fatigue crack growth in guide rails of launcher 71032-012 tested in the laboratory. (a) initial cracking in service, (b) Nz spectrum factored by 3.0, (c) final stages of cracking with spectrum factored by 2.5.....	39
Figure 19. Fatigue crack growth from an EDM notch in the guide rail (inset) of launcher 0175. The delineation between the melted grains of the notch and the sharp edges of the striation crack growth is difficult to discern.	40
Figure 20. Strain results from the strip gauge on the upper rail during snubbing and subsequent down loading to 5.95g (Experiment 7). The two peaks at gauges B and H lie either side of the line of extension of the crack.....	41
Figure 21. "Load shedding" as seen by comparing the strip gauges (average of E, F and G) at the forward hanger with the single gauges at the mid and aft hangers. These strains are from the loaded rail in Experiment 27.....	41
Figure 22 (a). The effect of the crack on strains in the guide rail : Strip gauge strains at the forward snubber on the cracked lower rail during 8.5g up loading of Experiment 5.	42
Figure 22 (b). The effect of the crack on strains in the guide rail : uncracked lower rail during up load of Experiment 20.	42
Figure 23. Crack growth in the guide rails of launcher 0148 from laboratory fatigue test.	43
Figure 24. Dark debris particles deposited on the fin as a result of wear at the aft hanging bracket during fatigue testing.	43
Figure A1.1. Flight measured launcher accelerations. [5].	54
Figure B2.1. The original Eddy Current technique as used by the RAAF. (from [1] AESF)....	58
Figure B2.2. The outboard corner reflection measured by a correctly positioned ultrasonic probe. This new technique was developed at AMRL [3].....	58
Figure B2.3. The reflection from crack (or artificial defect), within the gate, and outboard corner reflection.....	59
Figure B2.4. Cast shoe for correct positioning of the probe.	59

1. INTRODUCTION

A fatigue cracking problem associated with the guide rails of the LAU-7/A launcher (the term "launcher" is used to describe this component throughout this report) used on the F/A-18 has been reported by the Royal Australian Air Force. The results of preliminary investigations by the RAAF^[1] and AESF^[2] suggested that, because of the manner in which the launchers are utilised on the aircraft, large loads associated with carriage of the AIM-9 missiles may be causing the cracking of the guide rails. The problem appeared to be compounded by the fact that the aft snubbing of the missiles was often ineffective and appeared to result in the movement of the missile in the guide rails during carriage. The two factors were thus considered to result in the fatigue cracking of the guide rails at the location of the forward missile hanging bracket. It has been suggested earlier that the fatigue cracks grow under a high load/low cycle regime^[2].

The LAU-7/A launcher is attached horizontally to the wing tips of F/A-18 aircraft, Figure 1, unlike its previous applications (e.g. the MIRAGE) where it was attached vertically to the underside of an aircraft wing. Thus, with the present usage conditions on the F/A-18 aircraft, under positive g the upper guide rail of the launcher experiences a significant moment from the missile, and higher loads are being generated in the guide rails in this configuration. Although the USN F-14 also uses AIM-9 sidewinders in the side mounted orientation, the pylon is on a fuselage station and does not see the dynamic loading environment of the F/A-18 wing tip.

A section through the AIM-9 missile, hanging bracket and LAU-7/A launcher guide rail in the region of the forward hanging bracket is shown in Figure 2. The launchers are extrusions of 2024 aluminium alloy in the T8511 heat treatment condition. Most of the housing wall is of uniform thickness, however in the forward region some machining has been undertaken to increase the internal volume of the housing. The guide rails are on the outer surface of the launcher, Figure 2, and the missile hanging brackets engage the rails at the three locations shown in Figure 1. Snubbing is provided at the aft and forward locations in the guide rails. The aft snubbing is provided by a scissors arrangement, the blades of which engage the hanging bracket lug which then forces the bracket outwards against the inside of the guide rail. The forward snubbing is accomplished by machined steel plates which move (edgewise) onto the forward missile hanger and lock it in the guide rail to prevent lateral and vertical movement of the missile. The edges of these plates are seen in Figure 3, which shows the forward snubber area. The missile is held in the launcher by a detent mechanism activated by leaf springs. The detent must be applied during installation of the missile and is, itself, released on the firing of the missile by the forward thrust of the missile motor. Many of the hanging brackets, both forward and aft, removed from

¹Aircraft Engineering Support Facility, Highett (Vic), formerly Quality Assurance Laboratories.

missiles which have been in service for many months show wear and likewise the launcher guide rails show wear.

The location of the fatigue crack is shown in Figure 4 and a typical fracture is shown in the inset figure. Left and right-hand sides of the launchers are also defined in Figure 4. At overload failure, when the fatigue cracks have attained critical length, the fatigue cracks are generally of high aspect ratio typically 40 mm along the length of the guide rail and 1 to 3 mm deep. The shallow nature of the cracks creates some considerable difficulty in the inspection of the guide rails. In conjunction with NDISL², No. 481 Wing has developed a new NDI technique which, within the limitations discussed in Section 5.6 of this report, appears satisfactory for the inspection of guide rails. The previous standard technique and the inexperience of operators led to some inaccurate reporting of crack lengths and, possibly, over-estimation of the numbers of launcher guide rails which had cracked in service.

From a metallographic examination of a launcher failed in service, [2] it was apparent that cracking initiated as a result of the stress raising effect of the sharp radius under the lip of the guide rail. This is shown in Figure 5 (after [2]), where it can be seen that initiation of cracking is at a number of sites. The presence of small, intermetallic particles near the surface possibly aided the initiation of cracking. The preliminary scanning electron microscopy has shown that sub-critical crack extension occurred by fatigue. Within this region there was evidence of frequent over loads (causing patches of dimpled rupture) and regions of striation crack growth typical of fatigue. Final fracture by microvoid coalescence (overload) occurred when the crack had grown to a depth of 1 to 3mm, see Figure 6.

The RAAF inspection method was applied to all launchers during their 50 hour refurbishment, and a rejection criterion of a crack length of 20 mm was applied to the launchers. This meant that launchers with cracks in the guide rails of greater than 20 mm could not be used for the carriage of AIM-9 missiles.

Information from other operators of the F/A-18 aircraft was limited, but did not suggest a problem which was as wide-spread as that reported by the RAAF. The Canadian Forces had reported some cracking in the forward hanging bracket region and had devised an additional load transference device to reduce the load at the hanging brackets. The disadvantage of this solution to the launcher cracking problem is that the launcher is no longer functional and hence, it can only be applied to aircraft used for training. There were no incidents of launcher guide rail cracking from the US Navy reported to the RAAF [3].

The reasons for the apparent excessive level of cracking in the RAAF fleet are unclear. It is possible that the launchers experience more missile carriage hours than other operators due to a smaller inventory of launchers per aircraft. It is also possible that early RAAF flying produced a more severe loading spectrum than that of other operators. A study of loads experienced by the LAU-7/A launcher has been

² Non-Destructive Inspection Service Laboratories, RAAF, Amberley.

undertaken by the NADC [4]³. This NADC study suggested that the release of Mk84 bombs produces the conditions of very high g loads (in excess of 25 g) which could give rise to crack growth in service. This was first reported by van Dyken and Merritt [5], after conducting flight tests with instrumented launchers at the NWC China Lake in California. In the case of RAAF usage, the dropping of Mk84 bombs is an infrequent role of the aircraft and so crack growth must result from other loads.

In the context of RAAF usage, the numbers of missile carriage hours to rupture have been determined for some LAU-7/A launchers, although these data may be somewhat unreliable because of both inherent difficulties in the NDI of the launcher guide rails (see comments below) and only recent detailed logging of launcher usage. It was found that some of the launcher guide rails had very short times to failure; one as low as 234 hours and also a grouping of failures occurs around 350 hours. The recorded failures of some of the launchers are summarised in Table 1. Following the initial reporting of cracking, an attempt was made to monitor crack growth in launcher guide rails and thereby find a relationship between particular operational squadrons and fatigue life (time-to-failure). However, none was apparent [3] from the limited fatigue data available, as summarised in Table 2. From the observed fatigue life behaviour of the launcher guide rails in the total RAAF F/A-18 fleet, however, it appears that most failures of the launchers occurred soon after the introduction of the aircraft into service when it was found that aircraft usage was most severe [6a,b]. Squadron-level fatigue monitoring procedures have since resulted in less severe flying with a concurrent reduction in fatigue cracking in the LAU-7/A guide rails. It is also possible that the reduction in rejection rate of the launchers in more recent times could be related to improvements in the NDI methods.

It is interesting to note that during the comprehensive US Navy program of environmental testing of the LAU-7/A [7,8], where launchers were subjected to a simulated 6000 hour life-cycle exposure (including a vibration and shock loading environment), no cracking of the guide rails was detected. The report, however, considered that, because of the way in which the loads were introduced into the launcher, the presence or absence of cracking cannot be considered indicative of service behaviour. The main objective of the test was the fatigue testing of the launcher components, such as the mechanism assembly and nitrogen receiver assembly.

The problem of ineffective snubbing and its significance in the overall fatigue cracking problem was investigated. While it was claimed by the RAAF operators that AIM-9 missiles could be moved easily in the launcher guide rails after snubbing (i.e. the snubbing is ineffective), the contribution of this movement to the observed short fatigue life was not known. The easier and more extensive movement at the rear suggested to the RAAF the hypothesis that supporting loads were being "shed" from the aft snubbers and taken by the tighter forward snubbers. This hypothesis was investigated.

Severe wear to the aft snubbing scissors has been observed, Figure 7, as has the wear to the aft hanging brackets seen in Figure 8. Wear has also typically been reported on the

³(US) Naval Air Development Center, Warminster.

guide rails at the location of the missile forward hanging brackets, Figure 9, and to the missile forward hanging brackets. These types of damage all suggested appreciable movement of the missile during carriage, but there was no evidence to suggest that the cracking in the forward region of the guide rail was initiated by the wear, see also Reference 2. In fact Figures 5 and 9 show that the crack initiation sites are remote from the wear marks produced by the hanging brackets.

In an attempt to overcome the problem of ineffective aft snubbing and presumably decrease load shedding to the region of the forward hanging bracket the RAAF has designed a wearplate which is inserted under the aft snubbers thereby increasing the wedging forces and reducing missile movement, Figure 10. The effect of this plate on the strains at the forward hanger was investigated. Similarly, in an attempt to decrease the loads at the forward hanging bracket, the Canadian Forces have designed sets of teflon cylinders to react aircraft loads directly onto the launcher housing rather than through the guide rails, Figure 11. As an aside in the project this configuration was also investigated in the strain surveys.

2. OBJECTIVES

The objective of this work was to determine the magnitude of operational loads and their effect on the fatigue behaviour of LAU-7/A launchers on Australian F/A-18 aircraft. This was undertaken by:

- a. Determining the mechanism for the initiation and propagation of fatigue cracks in the guide rails at the location of the forward missile hanging bracket.
- b. Determining the magnitude of load shedding to the forward hanging bracket location due to ineffective aft snubbing and whether or not this is a significant contributing factor to the observed fatigue cracking problem.
- c. Investigating the effectiveness of the proposed RAAF wear plate modification to the aft snubbing mechanism in restoring over-all missile clamping in the launcher rail at both hanging bracket locations.
- d. Conducting a fatigue testing program, using a loading sequence derived from RAAF F/A-18 flight data, to determine if high N_z loads contributed to the observed fatigue cracking problem. In addition, this work would also provide guidance for a fatigue testing program to verify the effectiveness of any repairs to the launcher guide rail.

3. EXPERIMENTAL METHODS

3.1 Fractography of LAU-7/A Launcher Housings

Two fracture surfaces from failed LAU-7/A launcher housings were examined using a scanning electron microscope. The surfaces were taken from launchers 0217 and 0355. The fracture surface from launcher 0217 was of particular interest because this rail failed in 234 hours, see Table 1. This was considered by the RAAF to be an extremely low number of missile carriage hours. Unfortunately, as overload occurred while the missile was being carried, some damage was sustained by the fracture surface with the result that the initiation point was not preserved on the surface.

Scanning electron microscopy was also used to study the fracture surfaces of launcher guide rails fatigue tested during the course of this investigation.

3.2 Static Strain Surveys

This work involved the use of a launcher and dummy AIM-9 missile to determine experimentally, using strain measurements, the load shedding to the forward hanging bracket location as a result of ineffective aft snubbing. For this work LAU-7/A launcher serial number NMH 230 was used. Prior to testing, this launcher was inspected by an NDISL eddy current technique, see Table 3. The left-hand guide rail gave strong indications of the presence of a crack of approximately 20mm while the opposite guide rail was found to give a small, but inconclusive indication of a crack. The launcher was strain gauged at the three hanging bracket locations. The locations of the strain gauges are shown in Figure 12.

A rig was constructed for the experimental loading program and is shown in Figure 13. The loads were applied through the centre-of-gravity of the dummy missile using a hydraulic actuator acting through a specially designed load carrier. Figure 14 shows a tail view of the launcher mounting position that is obscured by the missile in Figure 13. The static loads for the strain surveys were applied using a simple hydraulic hand pump, seen in Figure 13, driving the actuator.

The peak load applied was drawn from the N_z spectrum of flight loads data from aircraft A21-015. Initially, the peak static loads applied in the test simulated the peak 8.5g inertial load downwards and 8.5g upwards. See Appendix A for the relationship between g and actuator load in kN. In these (initial) experiments there was *no factoring* of the N_z loads to take into account dynamic effects. The test loads were applied stepwise in increasing and decreasing 1g steps to the peak N_z . The launcher guide rail was tested in two orientations; cracked rail up and cracked rail down. The static loading program is summarized in Table 4. This program also covered a range of missile installation configurations.

Two of the installation conditions were "supported" and "unsupported" snubbing. During supported snubbing the weight of the missile was taken by a crane during installation. In other experiments the missile was allowed to hang under its own weight (i.e. unsupported) in the launcher rail. In the supported case the aft snubbers

were engaged when the aft hanger was positioned midway between the upper and lower launcher rails, whereas the unsupported snubbing allowed the hanger to rest on the lower rail. These conditions were trialed in order to determine if more effective snubbing could be developed by supporting the missile during snubber engagement and whether lower strains resulted at the forward hanging bracket.

Other installation configurations investigated were with worn aft snubbers and bent clevis arms in the aft snubbing mechanism. A bent clevis results in uneven snubbing forces which allow greater movement of the missile.

Once the level of load shedding had been investigated, the effectiveness of the RAAF wear plate addition to the aft snubbing device was tested. Loading experiments, similar to those used above, were conducted on the system with the RAAF wear plate attached, as in Figure 10.

The teflon cylinders introduced by the Canadian Forces were replicated and trialed in just two experiments. The configuration is seen in Figure 11 from [9]. One set of cylinders was adjacent to the forward snubbers and one set attempted to restrict missile vertical movement at the aft snubbers. The recommended torque settings were used, but re-torquing was required after only a few high load cycles as the teflon deformed.

To investigate the possible contribution from airloads on the missile fins a steel torque strap was fastened to the extremities of three fins and dead weights applied to twist the rear of the missile in the launcher as seen in Figure 14. The direction of twist was consistent with the lift on the fins that results from the impingement of the wing tip induced vortex on the fins: i.e. rotating the missile inboard. The dead weight loads were selected after calculating the airloads and performing a static strength assessment of the missile fins under the imposed loading. Clearly, the flow around the missile on the wing-tip is a complex field only quantifiable by a large research effort and that was not appropriate to this investigation. See Appendix A for a brief discussion of the loads used in the torque strap experiments. With the loading system used, the calculated static strength limited the maximum weight applied in these experiments to 280lb which gave a torque of 2646inlb. This is only one fifth of the estimated maximum torque that could be developed by the fins at Mach 1.3.

3.3 Fatigue Test of LAU-7/A Launcher Guide Rails

Fatigue testing of several launcher guide rails was undertaken using the same loading train as that used for the static loading experiments, but for these experiments the actuator was driven by a closed loop controlled servo-valve commanded by a computer. The computer generated loads using a sequence (LAUSEQ) derived from the flight loads data of aircraft A21-015⁴. The load sequence derived from the MSDRS vertical acceleration records of this aircraft represented approximately 191.8 hours of flying. Details of the sequence used for this testing program are given in Appendix A.

⁴ Launcher number 0217 was carried exclusively on this aircraft and one of the fracture surfaces studied in the present work was from this rail.

The sequence represents usage of the aircraft from approximately 2 February to 30 September 1987. This was the period during which launcher guide rail 0217 failed and it was considered that this sequence represented the "severe" flying during the early stages of RAAF operations with the F/A-18. A dead band in the 3 to 4 g range exists for these data, but this was considered not to influence fatigue life since fractography has shown that the loads which produce most of the fatigue cracking are likely to be the high g loads, see Section 4.1.

The sequence was run at approximately 0.4 Hz (average frequency) and peak loads were monitored using a chart recorder. Initially the peak down load applied was 8.7 kN which corresponded to an N_z of 8.07 g, but, after inspections revealed no crack growth, these loads were "factored up" to account for the dynamic loads experienced at the wing tip of the F/A-18 aircraft. As far as we know, the magnitudes of these loads have not been measured on RAAF F/A-18 aircraft, but some indications of expected loads can be gained from other studies [10 - 11]. Typical carriage accelerations are summarised in the Tables A1.1 and A1.2 in Appendix A. The highest launcher accelerations shown in these tables of flight measurements are over three times the N_z limit of the F/A-18. As a result the fatigue spectrum peak load was incrementally factored up to 3 times the nominal value until crack growth was achieved at similar rates to service usage. All loads in the fatigue sequence were consequently factored up by this amount.

The launchers were fatigued for 50 spectrum flying hours and then inspected for evidence of cracking. The inspections used the methods described in Section 3.6 and Appendix B. Fractographic evidence from fatigue tested launchers was also used to confirm that the crack growth rates were similar to launchers with service failures.

3.3.1 Preliminary Fatigue Test of Launcher 0148 (RH Rail)

Preliminary fatigue testing was undertaken on launcher 0148. The left-hand guide rail, when inspected prior to fatigue testing, was found to have a crack of 39mm and the right-hand rail gave only inconclusive evidence of cracking, see Table 3. The launcher was mounted with the right-hand rail uppermost and the spectrum applied with the loads predominantly in the downward direction. This induced cracking of the upper (RH) guide rail, but to achieve crack growth the loads were "factored" by initially 1.2 and then later in the test by 2.0.

One problem encountered in this preliminary test and in subsequent fatigue tests was the re-distribution of loads during testing. Strains at the upper cracked rail were reduced by approximately 15% as is illustrated in Figure 15 for launcher guide rail 0148. This appeared to have arisen from minor dimensional changes in the guide rail associated with cracking and from wear of the guide rails; thus loading was transferred to the edge of the lower guide rail during testing. To overcome this problem shims up to 0.9mm thick were inserted between the hanging bracket and the contact point on the upper guide rail thus restoring strains in the rail to the higher, earlier values. This is illustrated by the graph of Figure 15 for launcher guide rail number 0148.

Crack length was monitored by two methods; eddy current (applied at the inner section of the guide rail) and ultrasonics (applied at the outer surface of the guide rail); see Appendix B.

3.3.2 Fatigue Test of Launcher 71032-012 (LH Rail)

This launcher was inspected by both NDISL eddy current and AMRL ultrasonic methods. A 43 mm crack was found in the right-hand guide rail, whilst for the LH rail the eddy current method gave inconclusive evidence of cracking and the ultrasonic method gave no indication of cracking in this rail, see Table 3. The "uncracked" (LH) guide rail was mounted uppermost and the load spectrum applied as described above. Again it was found necessary to "factor" the N_z loads by 2.0 to induce crack growth.

3.3.3 Fatigue Test of Launcher 0715 (LH Rail)

This launcher had a failed RH guide rail and, using the AMRL ultrasonic method the LH rail gave no indication of the presence of a crack. The failed guide rail was patched using a repair method developed at AMRL. The repair consisted of a machined fitting bolted to the side of the launcher housing in the area of the failure. The upper (LH) rail had a small crack electro-discharge machined (EDM) in the region of the forward hanging bracket. The rail was then fatigue tested using an N_z spectrum "factored" by 3.0. To ensure the rail was fully loaded the hanging bracket was locked into position with a 0.9mm steel shim.

3.3.4 Fatigue Test of Launcher 71032-012 (RH Rail)

A repeat fatigue test was conducted on launcher 71032-012, this test was on the cracked right-hand launcher guide rail. The failed LH rail was patched using the AMRL repair method. The cracked rail was mounted uppermost in the test rig and the hanging bracket fully shimmed. Again, the N_z spectrum applied through the missile was "factored" by 3.0.

3.4 Wear at Hanging Bracket Locations

During the course of testing wear at the forward and aft hanging bracket locations was monitored. This was simply visual observations of damage to the launcher guide rails, the hanging brackets and the snubbing devices.

3.5 Additional Failures

Since the method of applying the loads to the launcher guide rail was, of necessity, a simplified loading train, and therefore the loading environment did not accurately simulate the loading conditions in service, it was considered likely that additional failures of the system might occur. Inspections were carried out on the rig and the dummy AIM-9 missile. Bolt tensions in the launcher and the dummy AIM-9 were checked periodically throughout the testing program.

3.6 Non-Destructive Inspection of Launcher Guide Rails

The launcher guide rails were inspected initially by an eddy current method developed by NDISL. This method, described elsewhere [11], required that the missile be removed from the guide rail for each crack length determination. An alternative technique was developed at AMRL and was based on a Canadian inspection technique using ultrasonic signals, see Appendix B and Reference [12]. This method did not need the missile removed from the guide rail since the inspection was carried out from the outer surface of the rail.

An attempt was made to check the accuracy of the ultrasonic method against the NDISL eddy current method used by the RAAF. A summary of the NDI of the launcher guide rails performed at AMRL is given in Table 3. It can be seen from Table 3 that consistent crack sizing of guide rails containing fatigue cracks is not achieved and so further refinements of the launcher guide rail inspection methods are desirable, see Section 5.6.

4. RESULTS

4.1 Fractography of LAU-7/A Launcher Housings

During the course of this work fracture surfaces were cut from failed launcher guide rails and examined in a scanning electron microscope. The fracture surfaces derived from service failures were minimally cleaned using acetate stripping. Sufficient areas of good quality were found to assess the crack growth mechanisms operating in service.

4.1.1 Service Failures

Fracture surfaces from launchers 0217 and 0355 were similar, with fatigue striations in evidence on the surfaces, see Figures 16 and 17. An interesting and important feature of the fracture surface was the presence of bands of ductile tearing associated with subcritical crack growth. This feature occurred irregularly throughout the regions of striation crack growth. A similar feature was observed on the fracture surface of the bulkhead material (7050 T7651) of the F/A-18 which had undergone laboratory fatigue testing under the MCAIR 300 hour block [13]. In the case of the present work, it appears that the wing tip of the aircraft was subjected to loads which produced regions of ductile tearing during the life of the LAU-7/A launcher guide rail. It has been suggested [3], that high g loads are generated with Mk 84 bomb drops. However, given the frequency of these regions of ductile tearing on the surfaces of guide rails 0217 and 0355, it was *not* possible to associate these with bomb drops from RAAF aircraft.

In the case of the fracture surface from launcher number 0217 (flown on aircraft A21-015) an average of approx 900 striations per mm was determined for the regions of fatigue crack growth. If the crack growth rate is assumed constant over the surface it was estimated that, for this launcher, crack extension events occurred at the rate of 6.2 events per missile carriage hour. This rate of crack extension is too slow to be caused by the aerodynamic buffet loads or wing vibrations; it is more likely that crack extension occurs under the high N_z manoeuvering loads. These results accord well with the observations reported in [2] for the fracture surface from launcher 0159 and based on these observations the fatigue crack was considered to grow in the high load/low cycle regime.

4.1.2 Test Failures

The fracture surface from the preliminary fatigue test on guide rail 0148 showed regions of striation growth and tearing. However, the regions of tearing did not appear to be in the pronounced bands that were observed for the service failures 0217 and 0355. This laboratory specimen (0148) initially had only N_z loads applied (i.e. no factoring of loads).

The fracture surfaces from the laboratory tests on launchers 71032-012 and 0715, however, exhibited some areas of the banded structure on the fracture surface, similar features to those of surfaces taken from the service failures. The regions of tearing corresponded with periods in the test where the N_z loads were "factored" by three (X3.0). This suggested that there were loads in the sequence which produced pronounced regions of ductile tearing (stable crack growth). Typical fracture surfaces are shown in Figures 18 and 19.

4.2 Static Strain Surveys

The static strain survey involved thirty different experiments as shown in Table 4. After the first five experiments, the maximum load level was decreased to 70% of 8.5g to conserve the important asset of the instrumented launcher. The load levels causing fatigue crack growth were uncertain at that time. After the fatigue test program demonstrated substantial fatigue life and residual static strength at three times the initial peak load level, a follow-on series of static experiments gathered strain data up to the 300% level. Note that initial difficulties with the data acquisition equipment caused the loss of data from Experiments 1 and 4.

Strip gauges proved useful in detecting the peak strain lobes on the outer rail surface. These lobes occurred either side of the line of extension of the crack. Figure 20 shows the strains measured by the strip gauges for the uncracked rail of Experiment 7.

Figure 20 illustrates the various stages of the snubbing procedure and the strain response of the strip gauge on the upper rail as down loading is increased. Engagement of the forward snubbers produces no noticeable strain in the rail at any location, since the missile weight was at that time supported by the crane. Removing the crane after snubbing and allowing the 1g weight to rest on the launcher produces strain per g increments (-85 $\mu\epsilon$) slightly greater than those for the 5.95g down load (-410

$\mu\epsilon$). Removal of the support allows the missile to settle onto the lower rail thus changing the load paths and producing the small initial non-linear increase.

The single axial gauges at the mid and aft hanger locations are not directly comparable to the strip gauge readings across the varying strain field. However, the gauges 1 through 8 are of 3mm gauge length and their positions correspond approximately to the positions of gauges E, F and G in each of the strip gauges.

Accordingly, Figure 21 shows a strain comparison from Experiment 27 where the strip gauge results are presented as the average of those three gauges. The maximum load was a 24g download. The strains remain essentially linear above 1g and in the same proportion indicating small load path changes are confined to the low g region.

Comparison of the average of the strip gauges 9E, 9F and 9G with the adjacent axial gauges (1 and 2) at the forward hanger shows that there is a peak strain near the centre of the forward hanger location. Since gauge 1 (fwd) is initially slightly greater than gauge 2 the longitudinal peak is just in front of the centre of the forward hanging bracket location. In all of the figures showing fracture surfaces, the location of the maximum depth of crack is slightly forward of the central position. The strain readings are consistent with this observation.

The aft strain gauges in Fig. 21 show much lower strains than the forward. This observation is common to all the experiments performed, with maximum load strains typically less than -200 to -350 $\mu\epsilon$ when the comparable strain at the forward hanger is between -900 and -1000 $\mu\epsilon$. Additionally, the maximum strain observed for the aft strain gauges 7 and 8, (-350 $\mu\epsilon$) was recorded in this experiment (27) with a down load equivalent to 24g. The corresponding peak strain at the forward hanger was approximately -2000 $\mu\epsilon$ (9H) indicating that the rail at the aft hanger was a less significant load path than the rail at the forward hanger.

The presence of a crack adjacent to the forward snubbers appears to significantly increase the strain measured on the outer surface of the rail. The effects of rail cracking are summarized in Figure 22 from Experiments 5 and 20. Figure 22(a), from a cracked rail, shows a peak strain recording of approximately -910 $\mu\epsilon$, whilst Figure 22(b), from an uncracked rail, shows only -370 $\mu\epsilon$. Since the up load in Fig. 22(b) is half that of (a), the strain can be doubled to -740 $\mu\epsilon$. Comparison of (a) with (b) then shows that the crack has produced an increase of 23% in the peak strain.

One of the other main issues addressed in this work is whether worn aft snubbers increase the strains at the forward hanging bracket location. Table 5 shows clearly that the opposite is true. Independent of the snubbing procedure the new scissors result in strains 35 to 50% higher at the forward hanging bracket. The single gauges show the same effect as the strip gauges, confirming the validity of the readings. The strain at the mid hanger rail is insignificant and shows no effect of snubber wear. However, the strains recorded at the aft hanger complicate the picture of the load paths. Gauge 7 recorded a strain of -140 $\mu\epsilon$ with worn aft snubbers and only a nominal strain with new aft snubbers. The gauge on the lower rail (8) shows insignificant strains during down loading for both cases. This clearly indicates that with new aft snubbers the aft load

path is almost entirely through the snubbing scissors and snubbing bar, but not through the rails.

Additional evidence of this result is seen in Table 6 which shows the difference between total movement at the forward hanging bracket for worn and new snubbers. The extensometer was positioned to read the relative vertical displacement between the launcher body and the forward hanging bracket. The two experiments using worn aft snubbers showed up to 5 times greater total displacement than the corresponding experiment with new snubbers. Movements of the order of 1mm are not due to strain in the rail, but to movement from rail to rail as observed and noted during the load application runs.

Table 5 also presents examples of the experiments performed to show the effects of snubbing procedure on strain levels at the location of the forward hanging bracket in relation to the condition of the aft snubbers. For new aft snubber scissors the procedure makes no appreciable difference. However, for worn snubbers, supporting the missile weight during snubbing increases the 1g strains at the forward hanger compared with unsupported snubbing. The strain difference does not occur when the forward snubbers are applied, but when the crane support is removed the strains increase from very low values to approximately $100\mu\epsilon$. This is effectively a pre-strain due to the changes in detailed geometry of the forward hanger contact areas introduced by ensuring that the forward hanger is aligned correctly before snubbing. Table 5 also shows that strains per g at the forward hanger due to supported and unsupported snubbing are increased by using new aft snubbers.

The effect of the steel wear plate under the aft snubbers is seen by the comparison of the results from the experiments shown in Table 7. The cracked rail shows a significantly greater strain at the forward hanger with the plate installed, which is consistent with the experiments using new aft snubbers. However, for the uncracked rail, Table 7 shows that the critical delta strains are reduced by installing the wear plate.

The effects of the torque strap are not surprising as seen in Table 8. With increasing inboard torque, load is transferred from the upper rail to the lower rail. The strain distribution around the forward hanging bracket is quite different to that for the inertia loads. The peak strain occurs at the forward gauge on the lower rail and is 25 to 50% higher than those of the corresponding strip gauge peaks. This strong bias towards the forward gauges is not representative of the loading that produced the observed fatigue crack surfaces of the in-service failures. The maximum depth of crack in all cases was only slightly shifted forwards of the central hanger position. Strain distributions for the inertia load cases show that the peak strain would correspond with this position. The torque strain distribution would produce a maximum depth of crack close to the forward gauge position. Torque loading is therefore, not the dominant loading in the observed failures.

The results of the experiments with teflon cylinders are presented in Table 9. At the forward hanger on the most highly loaded rail the strains were, surprisingly, approximately 10% higher with the cylinders installed than on equivalent experiments with no cylinders. The teflon cylinders appear to wedge the AIM-9 away from the

LAU-7/A, causing the additional strain. The strains at other locations were reduced and even changed in sign.

As evidence of this, consider the 1g strains of the upper rail (peak of $-199\mu\varepsilon$) which are much greater than without the cylinders ($-110\mu\varepsilon$). After subsequent load application cycles, hysteresis is seen in that the 1g strains (peak) stabilize at approximately $-540\mu\varepsilon$. This indicates the progressively increasing wedging action of the teflon cylinders. The trend with increasing down load is that the delta strain is decreasing. If the trend continues, at loads a few g above the 5.95g down load of these experiments, the teflon cylinders will reduce the absolute peak strain in the rail. This is a reduction in strain per g. Since the 1g strains are significantly increased the mean strain would also be increased. However, the benefit is that the cyclic component of the strain may well be reduced and the fatigue life extended.

4.3 Fatigue Behaviour of LAU-7/A Launcher Guide Rails

4.3.1 Preliminary Fatigue Test of Launcher 0148 (RH Rail)

This preliminary fatigue testing was undertaken to gain some idea of the effectiveness of the test method and to discover any problems with applying the loads through the C-of-G of the dummy missile. The launcher was mounted with the cracked rail down and N_z spectrum loads were initially applied (8.07g in the downward direction). The rail was inspected for cracking approximately every 50 hours of spectrum flying, and under the unfactored N_z loads there was no recorded crack growth over 20 loading programs (3836 hours of flying). The N_z load spectrum was then "factored" by 1.2 in an attempt to induce cracking in the upper guide rail. No crack growth occurred during the application of a further 14 loading programs. The (original) N_z loading sequence was then "factored" by 2.0 and during the application of these additional loading programs some crack growth was recorded. Between programs 20 and 37 at this load level, however no crack growth was recorded and this was found to be due to a load redistribution in the system as discussed in Section 3.3.1 above, see also Figure 15. Wear of the upper guide rail resulted in the hanging bracket loading the lower guide rail, thus reducing the applied loads to the upper rail. This was overcome by shimming the launcher hanging bracket in the upper guide rail, whereupon higher strains (loads) were restored to the upper guide rail. Failure of the upper guide rail occurred after a further 30 loading programs.

4.3.2 Fatigue Test of Launcher 71032-012 (LH Rail)

For the fatigue test of this launcher the initial loading programs applied to the upper guide rail used N_z loads which were "factored" by 2.0. Crack growth was found to occur rapidly in the first 5 loading programs and then stopped for a further 3 programs. Loads "factored" by 3.0 were then applied and crack length increased to 40mm by the completion of program 12. The loads were then "factored" by 2.5 and crack growth to a total of 43 mm was measured at the completion of program 28. It was expected that the fracture surface of the guide rail would be "marked" by this process thus enabling the regions of high loads to be identified. Fatigue loading was

continued using a load spectrum with N_z loads factored by 2.0. During this period of fatigue loading it was found that crack growth slowed and this was found to be caused by load shedding as observed in the preliminary fatigue test described in Section 4.3.1, above. Rapid crack growth occurred once a shim was installed at the forward hanging bracket location. The crack growth behaviour for the upper guide rail of launcher 71032-012 is plotted in Figure 23.

4.3.3 Fatigue Test of Launcher 0715 (LH Rail)

This launcher had one guide rail failed and the other gave no indication of cracking. The lower rail was patched [11] and the upper rail was machined with a small crack in the region of the forward hanging bracket. The rail was then fatigue tested using an N_z spectrum "factored" by 3.0. To ensure that the rail was fully loaded the rail was shimmed with a 0.9 mm shim. Fatigue failure occurred within the 6th loading program.

4.3.4 Fatigue Test of Launcher 71023-012 (RH Rail)

This test was a repeat of the fatigue test in Section 4.3.2 above, but for the other rail. The growth of the fatigue crack is shown in Figure 23.

4.4 Movement and Wear at Hanging Bracket Locations

During most of the fatigue tests wear debris accumulated at the aft snubbing location. This was further evidence that the aft snubbing was ineffective. Figure 24 shows the wear debris accumulated on the fins of the dummy AIM-9 missile during fatigue testing.

4.5 Additional Failures

During the course of the fatigue testing of the launcher guide rails several failures of the (upper) forward hanging bracket attachment bolt (NAS-1219-5EP) on the dummy AIM-9 missile occurred. The fatigue crack was initiated at the base of the driver slot and progressed downwards to the shank of the bolt and subsequent overload failure resulted in the shearing of the bolt head. The manual requires that these attachment bolts be tightened to a torque of approximately 10 Nm but it appears that this may not be sufficient for this application. Bolts which were not sufficiently torqued (say to 30 Nm) readily unfastened and subsequently failed in very few programs of loading. This unfastening of the upper hanging bracket bolt during testing also contributed to the load shedding observed in the experiments. It was found essential that the hanging bracket bolts be kept at a high torque during the fatigue test.

4.6 Non-Destructive Inspection of Launcher Guide Rails

As noted earlier in this report, two methods of NDI were used for the inspection for cracks in the launcher guide rails. As the testing program progressed only the

ultrasonic method was retained. Initially both methods were used for the inspection of cracks in the upper guide rail of launcher 0148 and as can be seen from Appendix B there was not always good agreement between the two methods. This is discussed in detail in Section 5.6. However, if one method only was used for a particular test, then indications of crack size were probably self consistent and hence gave reasonable measurements of crack growth. As the testing program progressed, the ultrasonic method was retained because of its convenience of use.

5. DISCUSSION

5.1 Static Strain Surveys

The investigations of the load shedding were to test whether additional loads were transferred to the forward hanging bracket as a result of ineffective aft snubbing. The results did not suggest that this occurred, since slightly higher strains were recorded for new snubbers rather than worn snubbers. The reasons for this are not discernible from these experiments. Other possible load paths are through the forward snubber plates or the launcher housing body between the rails. Worn aft snubbers allowed the rear of the missile to rest on the lower rail during unsupported engagement of the forward hanger. The slight variation in alignment and position of the forward hanging bracket introduced in this manner may increase the share of the load in the alternate paths. It was not possible to observe whether the alternate load paths transmitted the missile loads to the launcher rails through the snubber plates, rail edges or directly to the launcher body.

Similarly, the RAAF wear plate did not conclusively reduce the strain at the forward hanging bracket. The experiments presented in Table 7 appear to contradict each other on this matter depending on the presence of a crack in the loaded rail. The cracked rail was loaded by the up load during case A and the opposite for case B of Table 7. In each case the strains when a plate was present were increased by approximately 20 and 40% respectively. Conversely, when the uncracked rail was being heavily loaded, it showed strains lower by 14 and 70% respectively when a wear plate was installed. It is not possible from these results to conclude what mechanism is causing such a change in the load path in the presence of a crack. As such, these results cannot conclusively support the use of a wear plate to reduce strains at the forward hanger by greater aft snubbing.

Although variations in the position of the forward hanger during snubbing were minimized, slight changes occurred during loading that will transfer some of the load to the snubber plates or the lower rail. In particular, contact between a corner of the forward hanger and the base of the rail will transfer load to the lower rail without causing higher strain readings. This contact has been mentioned earlier as wear and indentations found at the base of the extruded groove in the rails of fatigue damaged launchers. Deflection of the missile under the applied loading will rotate the hanger to

cause contact. There is little other direct evidence of the changing load paths at the forward hanger, but the forward snubber plates may also be significant load carriers when the missile moves down to the lower rail.

5.2 Movement and Wear at the Hanging Bracket Locations

The results of the static loading survey have shown that the missile will move in the guide rails irrespective of the condition of the present snubbing system. This movement under load accounts for the wear imparted to both the forward and aft hanging brackets, the snubbers and the guide rails. It appears that the missile "loads down" on to the inner edges of the guide rails during flight thus producing wear in this region also. From the launcher and dummy missile system tested in the present work it appears that wear will always be a problem associated with this system and largely results from the unsymmetrical loading arising from the wing tip carriage of the system. A re-design of the aft snubbing system has been undertaken in an attempt to overcome some of the problems associated with the present scissors arrangement [14]. While, on the basis of the present experiments, a redesigned aft snubber system is unlikely to alter the load distribution in the launcher/missile system it may be possible to overcome the wear problem⁵.

Replacement of worn aft snubbers with new snubbing kits does not appear to solve the problem of wear at the forward hanger and indeed it appears that strains in the outer wall of the guide rail increase by some 20%. The reasons for this increase in strain with fitment of new snubbers is still undetermined, however the actual strains in the area covered by the strain gauge are small for the uncracked guide rail.

The Canadian Forces solution to the cracking problem which utilizes teflon cylinders bolted between the missile and the launcher housing clearly reduces the strain per g in the wall of the launcher at the location of the hanging brackets. However, AMRL considers it likely that creep in the teflon cylinders may reduce the beneficial effects over time. Furthermore, the solution does not allow the firing of the AIM-9 missile; it is strictly an interim fix.

5.3 Fatigue Crack Growth

The testing program has shown that fatigue cracking can be induced in LAU-7/A launcher guide rails by the application of an N_z load spectrum and that by "factoring" the load (by 3.0) it is possible to obtain crack growth rates similar to that measured in service. This suggests that some of the crack growth (at least) can be attributed to the inertial loads generated during missile carriage. The higher frequency vibrational loads were not simulated, but it is possible that these may also enhance crack growth, see [5],[7] and [8]. The use of "factored" N_z loads appears to be appropriate to the fatigue testing of LAU-7/A launchers. The fatigue striation count for the laboratory testing agrees well with the striation count for the service failures and again suggests that an appropriate sequence has been derived from a service aircraft.

⁵ The aft snubber mechanism was designed by Hawker de Havilland and has been evaluated by ARL [15].

The applied fatigue loads are larger than those resulting from vertical acceleration of the aircraft centre of gravity. It is not within the scope of this work to determine whether the additional loads result from asymmetric manoeuvres, aerodynamic loads on the missile fins or the wing tip vibration environment.

The presence of the bands of tearing on the fracture surface is often a feature of fatigue fracture surfaces and arises from the fact that, even for thick sections of some alloys, the material exhibits a rising R-curve and thus will sustain stable tearing at the high loads in a spectrum. This behaviour can be followed by further striation crack growth. Very similar behaviour has been observed, for example, on the fatigue fracture surface derived from the AMRL full-scale fatigue test of the F/A-18 488 bulk head [13].

The introduction of a shim at the upper forward hanging bracket location produced higher strains during fatigue testing, see Figure 15, and this appeared to be the result of small geometry changes in the forward hanging bracket region during testing. The small geometry changes may be attributed to wear of the upper guide rail and edges of the lower guide rail where the hanging bracket bears down under the test loading conditions. See Section 5.2 above.

5.4 Fatigue Behaviour of the Launchers

The static strain survey has shown that engagement of the forward snubbers produces a 1g prestrain in the rail. This small prestrain is 10 to 15% of the peak fatigue test strain that achieved crack growth at a similar rate to in-service failures. Ensuring correct missile alignment in the launcher by the use of supported snubbing produces only a 20% reduction in this pre-strain. Consequently, the influence of snubbing procedure on fatigue life is minimal.

It has not proved possible to reproduce total fatigue lives under laboratory conditions of the same order as that observed in service, despite approximately matching the crack growth rates in some areas of the crack. This has occurred for several reasons the most important of which are:

1. The applied spectrum is a "factored" N_z spectrum rather than a wing tip spectrum with vibrational loads.
2. The load is only applied at the missile centre of gravity rather than as a distributed inertia load, with some effect on the deflected shape of the missile.
3. There are small geometry changes in the system during fatigue testing which resulted in the shedding of loads to other parts of the system, thus decreasing the loads at the upper guide rail resulting in a slowing of crack growth. These loads can be restored during testing by shimming the hanging bracket in the guide rail.

Initial crack growth under the test conditions, however, appears to be similar to service crack growth in that it gives a projected failure rate of between 300 and 1000 spectrum hours, see Figure 23. It should be noted, however, that the vibrational loads seen by the AIM-9 and the launcher have not been included in this study and these may influence overall life. The overall fatigue-life exhibited by the launchers during testing is complicated by the load shedding which occurs during the program and so the

fatigue lives recorded in this work are not appropriate to the launcher. The use of shims to keep the load on the rail may only partially overcome the deficiencies of the present test system.

Testing with a vibration loads spectrum may provide additional information on the fatigue fractures observed in this launcher during service usage.

5.5 Additional Failures

The most significant additional failures observed in the present testing program have been the fatigue failures of the AIM-9 forward hanging bracket bolts. Similar failures have been reported during the vibration testing of a launcher housing and missile (conducted under the auspices of the RAAF) and some failures have been reported by PMTC [7]. The second group of failures has resulted in the specification of a substitute fastener for this application.

The only other "failure" observed during the testing program was the jamming of the detent mechanism making removal of the AIM-9 missile difficult at the conclusion of various stages of the testing. This problem did not inconvenience the work.

5.6 NDI Methodologies

The present work and the service inspection of the launcher guide rails has highlighted a problem in the application of NDI for a fitness-for-purpose inspection process. None of the methods used to date can be regarded as entirely satisfactory and it may well be that the present large number of guide rails rejected is the result of unreliable⁶ or inaccurate⁷ NDI techniques; neither limitation has been investigated fully. The eddy current techniques currently used by the RAAF and AESF often give indications of cracks when none is indicated by the AMRL ultrasonic test method, see Table B1.1, Appendix B. This may lead to an over estimate of the severity of the problem. However, it is also possible that the ultrasonic technique is not entirely reliable. Determination of the accuracy of each technique would require breaking open several fatigue-cracked launchers and checking crack length and depth against the NDI measurements. This would be a costly exercise which, in the present circumstances, would be hard to justify. It could perhaps be undertaken on launchers which have been written-off or classified as having cracks in excess of 20 mm. This would give a check of the methods for long cracks in the guide rails.

⁶ Both eddy current and ultrasonic techniques require operator experience to produce consistent detection of cracks.

⁷ Inherent inaccuracies within the NDI system.

6. CONCLUSIONS

The two problems associated with the LAU-7/A launcher housings which were studied in this work were:

1. Movement of the missile in the launcher housing during carriage on the F/A-18 and the possibility that this caused the transfer of excess loads to the forward hanging bracket location and
2. Fatigue cracking behaviour of the launcher guide rails in the region of the forward hanging bracket.

The results have shown that:

- a. whether the aft snubbers are new or worn does not prevent the missile from moving from rail to rail under high up and down loading, thus allowing the observed wear,
- b. the wear of the guide rail, hanging brackets and snubbers was due to movement of the AIM-9 missile in the guide rail during carriage and that this did not appear to increase loads in the guide rail at the region of the forward hanging bracket,
- c. the fatigue failure of the launcher guide rail in the region of the forward hanging bracket appeared to be (largely) due to high N_z loads.
- d. The influence of snubbing procedure on fatigue life is minimal and it appears that the hours in service of the snubbing kit has little effect on ability to restrain movement.
- e. The RAAF modification of adding a wear plate at the aft snubber does not produce a strain reduction in the rail adjacent to the forward hanger.

The present work also highlighted problems with the NDI methods used in the inspection of the guide rails both in service and in the experimental studies.

7. RECOMMENDATIONS

The initial recommendation of the RAAF, that the missile hanging brackets be flown until cracks reach a length of 20 mm is acceptably conservative. Launchers with cracks greater than this length are to be removed from service. Reinstatement of the launcher guide rails with cracks in excess of 20 mm necessitates repairs to the guide rails. Two methods should be considered:

1. Weld repair of the crack in the guide rail,
2. Machining-out of the cracked section of the guide rail and installation of a mechanical patch in the region of the forward hanging bracket.

Both of the recommendations for repair have inherent limitations which should be evaluated in a separate program, and this program should include extensive fatigue

testing of the repair(s). The "factored" N_Z spectrum investigated in the present work would be considered appropriate in the absence of a wing tip environmental spectrum. Further testing of repairs should be undertaken if such a spectrum becomes available; thus ensuring testing to the most severe operational condition.

8. ACKNOWLEDGEMENTS

The authors acknowledge the valuable discussions held with Sqdn Ldr D. Steer, Flt Lt C. Castles and Flt Lt J. Mitchell. The authors also thank WO W. Ealings for his assistance in obtaining components and drawings for the testing program. The authors acknowledge the co-operation and interest in this work shown by Mssrs C. Bott and M. Pekerinnen of AESF.

The authors would also like to acknowledge the assistance of Mssrs B. Bishop and H. Morton for their development of an NDI method for this work.

9. REFERENCES

1. RAAF Letter WEAP/4745/7336/4-15/1 (72) RESTRICTED
2. Quality Assurance Laboratories "Investigation of Cracked LAU-7/A-5 Launchers." Report No. NDT/94/87, October 1987.
3. Mitchell J. Private communication WEAP/4745/7336DOI-15/2 (31) enclosing unnumbered US Navy report.
4. Yankovich E. "LAU-7 Rail Structural Investigation". U.S. Naval Air Development Center, Warminster.
5. van Dyken R.D. and Merritt R.G. "AIM-9 Wing-Tip Carriage Aboard F/A-18, Flights Test Report" Vol. 1 and 2. Naval Weapons Center, China Lake, NWC TM 6108, Jan. 1989.
- 6a. Rider C.K., Higgs M.G.J. and Sanderson S. "Investigation of RAAF F/A-18 Service Usage 1985 (U)" DSTO, Aeronautical Research Laboratory, Aircraft Structures Division TM 499, November 1988 (Limited Release).
- 6b. Rider C.K., Higgs M.G.J. and Sanderson S. "Investigation of RAAF F/A-18 Service Usage 1986 (U)" DSTO, Aeronautical Research Laboratory, Aircraft Structures Division TM 501, January 1989 (Limited Release).
7. US Naval Air Systems Command "LAU-7/A Launcher Consolidated Environmental Envelope Program." Pacific Missile Test Center, Point Mugu, January 1985.

8. US Naval Air Systems Command "Final Report LAU-7/A Launcher Comprehensive Environmental Testing." Pacific Missile Test Center, Point Mugu, December 1989.
9. Canadian Forces "Special Inspection Instruction, LAU-7/A-5 and LAU-7/A-6 Missile Launcher Guide Rails For Cracks." National Defence, Canada C-75-290-000/NS-004, 1988-06-08, 1988.
10. Glasper D., Rodgers R., Heilman R. and Torres G. "LAU-127/A Integration Feasibility Study, F/A-18 Wing Tip Use of the LAU-127/A Launcher." Pacific Missile Test Center, June 1988.
11. RAAF NDISL "LAU-7/A Launcher - Non Destructive Inspection Procedure" STI - Armament Airborne Equipment / 196.
12. Bishop B. and Morton H. "Ultrasonic Inspection of LAU-7/A Launcher Guide Rail." DSTO Aeronautical Research Laboratory, Aircraft Materials Division TM 520, December 1989.
13. Barter S.A., Bishop B.C. and Clark G. "Assessment of defects in an F/A-18 FS488 Bulkhead Material" DSTO Aeronautical and Maritime Research Laboratory AMRL-MAT-R-125, August 1991.
14. van Blaricum, T.J. "LAU-7/A missile launcher static and dynamic strain surveys", DSTO Aeronautical Research Laboratory, Aircraft Structures TM 561, October 1992.

Tables

Table 1. Fatigue Failures of LAU-7/A Launcher Guide Rails

Serial No.	Flying Hours (hours of missile carriage)	CRACK SIZE length X depth mm X mm	AIRCRAFT
0159	334	42 X 1	A21-006
0217	234	43 X~1	A21-015
0715	357	53.5 X 5	various
0714	629	43.5 X 2.5	various
0355	no data	45 X 2	unknown

Table 2. Fatigue Crack Growth in LAU-7/A Launcher Guide Rails

Launcher Serial No.	Length of Crack when monitoring began (mm)	Launcher Air Frame Hours (hours)	Crack Extension (mm)	Location
001	14	44.2	5.5	77SQN
012	10	26.5	3.0	77SQN
0739	20	74.0	0.0	3SQN
0078	15	66.0	16.0	3SQN

Table 3. Crack Indications In Lau-7/A Launchers¹ Inspected At Amrl

Serial No.	RAAF ²		AMRL	
	side 1	side 2	side 1	side 2
71032-012	43	0	43	0 - 20
0148	36	0	39	9
0413	35	36	28	0
NMH-230	27	0	20	0 - 10

Notes:

1. No information as to the disposition of the cracks from RAAF NDI, hence the designations *side 1* and *side 2* for both sets of data.
2. These data from reference 7.

**Table 4. Summary Of Static Loading Experiments on LAU-7/A Launcher Housing S/N 0230
(Worn And New Aft Snubber Kits)**

Exp No	Crack in upper rail	Supported snubbing	Dial Gauge	Launcher Equipment					Loading	
				New Aft Snub	RAAF wear plate	CF teflon cyl	Torq strap	Fwd shims	Down (g)	Up (g)
1		#		Data	not	saved			8.5	
2		#							8.5	
3		#							8.5	
4		#		Data	not	saved				8.5
5										8.5
6									5.95	5.95
7		#							5.95	5.95
8		#		#					5.95	5.95
9				#					5.95	5.95
10				#	#				5.95	5.95
11		#		#	#				5.95	5.95
12		#		#					5.95	4.60
13	#	#		#					5.95	5.95
14	#	#		#					5.95	5.95
15	#	#		#	#				5.95	5.95
16	#	#		#					5.95	5.95
17	#	#		#	#				5.95	5.95
18	#	#		#	#				5.95	5.95
19	#	#		#					5.95	5.95
20	#	#		#					5.95	5.95
22	#	#					#		280lb	
23	#	#	#	#	#		#		280lb	
24	#	#		#	#	#			5.95	5.95
25	#	#		#		#			5.95	5.95
27		#		#					24.0	
28		#		#				#	25.9	
29		#		#						12.15
30		#		#				#		25.5

Notes:

1. supported snubbing utilizes a crane to support the AIM-9 missile during engagement and snubbing.
2. unsupported snubbing does not utilize a crane to support the AIM-9 missile after engagement.

Table 5. Comparison Of Strain Levels In The Uncracked LAU-7/A Launcher Guide Rail

		Supported Snubbing					
Snubbers	Worn	(Expt 7)		New	(Expt 8)		
Loads	Zero Crane off	Max -5.95g	Max-zero	Zero	Max -5.95g	Max-zero	
Gauge No. (Hgr)	$\mu\epsilon$	$\mu\epsilon$	$\mu\epsilon$	$\mu\epsilon$	$\mu\epsilon$	$\mu\epsilon$	$\mu\epsilon$
1 (fwd)	-174	-357	-183	-154	-417	-263	
9B (fwd)	-119	-430	-311	-98	-581	-483	
9H (fwd)	-132	-450	-318	-109	-609	-500	
2 (fwd)	-88	-378	-290	-71	-532	-461	
5 (mid)	-9	-17	-8	-9	18	27	
6 (mid)	-9	-123	-114	0	-116	-116	
7 (aft)	-9	-149	-140	0	-17	-17	
8 (aft)	0	26	26	9	18	9	
Unsupported Snubbing							
Snubbing	Worn	(Expt 6)		New	(Expt 9)		
1 (fwd)	-9	-146	-137	-155	-412	-257	
9B (fwd)	11	-316	-327	-109	-590	-481	
9H (fwd)	2	-336	-338	-132	-624	-492	
2 (fwd)	0	-308	-308	-62	-536	-474	
5 (mid)	0	-18	-17	0	18	18	
6 (mid)	18	-105	-123	-35	-177	-142	
7 (aft)	-9	-158	-140	-9	-26	-17	

Note:

1. All strains at the forward hanger are from the upper rail.

Table 6. Displacement Of The AIM-9 Missile Forward Hanging Bracket Relative To The LAU-7/A Launcher Housing

	Worn snubber kit Δz (mm)	New snubber kit Δz (mm)
CASE A no load (missile unsupported with no aft snubbing)	Experiment 19 0	Experiment 17 0
70% of 8.5 g down	0	-0.224
30% of 8.5 g up	0.889	-0.071
70% of 8.5 g down	0.114	n/d
TOTAL MOVEMENT (mm)	0.78	0.15
CASE B no load (missile snubbed with supported snubbing)	Experiment 20 0	Experiment 18 0
70% of 8.5 g down	-0.025	-0.31
50% of 8.5 g up	+0.864	-0.017
70% of 8.5 g down	+0.304	-0.381
50% of 8.5 g up	+1.06	n/d
TOTAL MOVEMENT (mm)	1.085	0.293

Table 7. Effect On Fwd Hanger Strains Of The Stainless Steel Wear Plate Modification To Aft Snubbers¹ Of LAU-7/A Launcher Number Nmh230

Experiment	no wear plate upper ² lower ²	with wear plate upper lower
CASE A missile snubbed cracked rail down no applied load 70% of 8.5 g down 30% of 8.5 g up	Experiment 8 -82 -13 -473 -14 0 -241	Experiment 11 -109 0 -444 -2 1 -276
CASE B missile snubbed cracked rail up no applied load 70% of 8.5 g down 30% of 8.5 g up	Experiment 16 -93 -18 -350 -37 -2 -202	Experiment 15 0 ³ -130 -463 -3 -2 -184

Notes:

1. new aft snubbers used for all experiments
2. strip gauges on the upper and lower rails presented as average of gauges E, F and G
3. This data suspect

Table 8. Strain Response To Missile Torque Load At The Forward Hanger For Normal Snubbing And With RAAF Wear Plate

Experiment No.	LOWER RAIL (Uncracked)		UPPER RAIL (Cracked)	
	Gauge No.	Delta Strain	Gauge No.	Delta Strain
22 (Normal)	1	-165	4	239
	9(E+F+G)/3	-130	10(E+F+G)/3	167
	2	-79	3	69
	7	-18	8	0
23 (Using RAAF wear plates)	1	-154	4	149
	9(E+F+G)/3	-17	10(E+F+G)/3	143
	2	8	3	173
	7	-79	8	0

Notes:

1. Delta strain is calculated from the difference between strain at maximum torque and at zero torque with the crane support for the missile removed.
2. Aft hanger strains without wear plate installed showed most strain response to dead weight of AIM-9, i.e. removal of crane support.

Table 9. Effect On The Strains At The Forward Hanger Of The Canadian Forces Teflon Cylinders As Additional Snubbers

Gauge No	NORMAL Experiment 18		TEFLON CYL. Experiment 25	
	0 kN	Max -4.1 kN	0 kN	Max -4.1 kN
1 9 (E+F+G)/3	32	18	0	18
	16	5	11	-3
	2	13	-18	-70
4 10 (E+F+G)/3	114	277	-301	-557
	220	526	261	-552
	35	216	-95	-472

Notes:

1. Both experiments with crack in upper rail, new aft snubbers and no RAAF wear plate

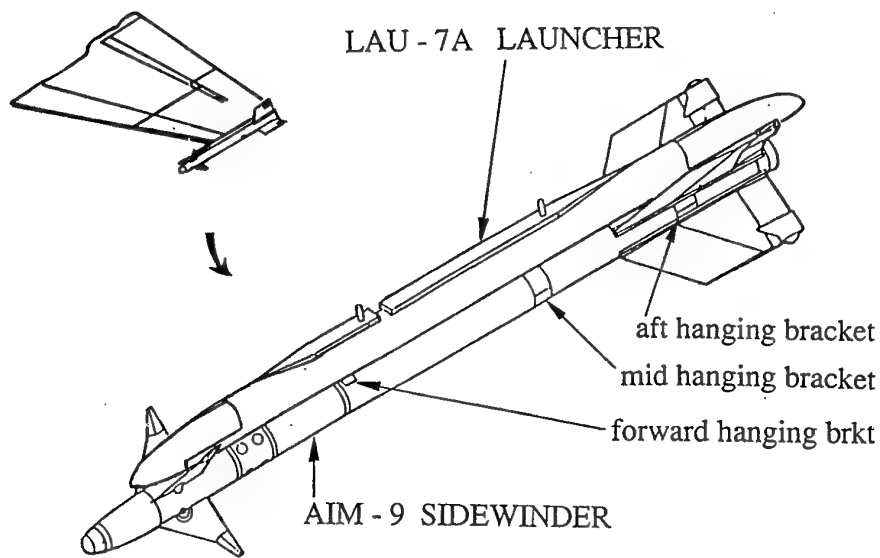


Figure 1. The wing-tip position of the LAU-7/A launcher and AIM-9 missile

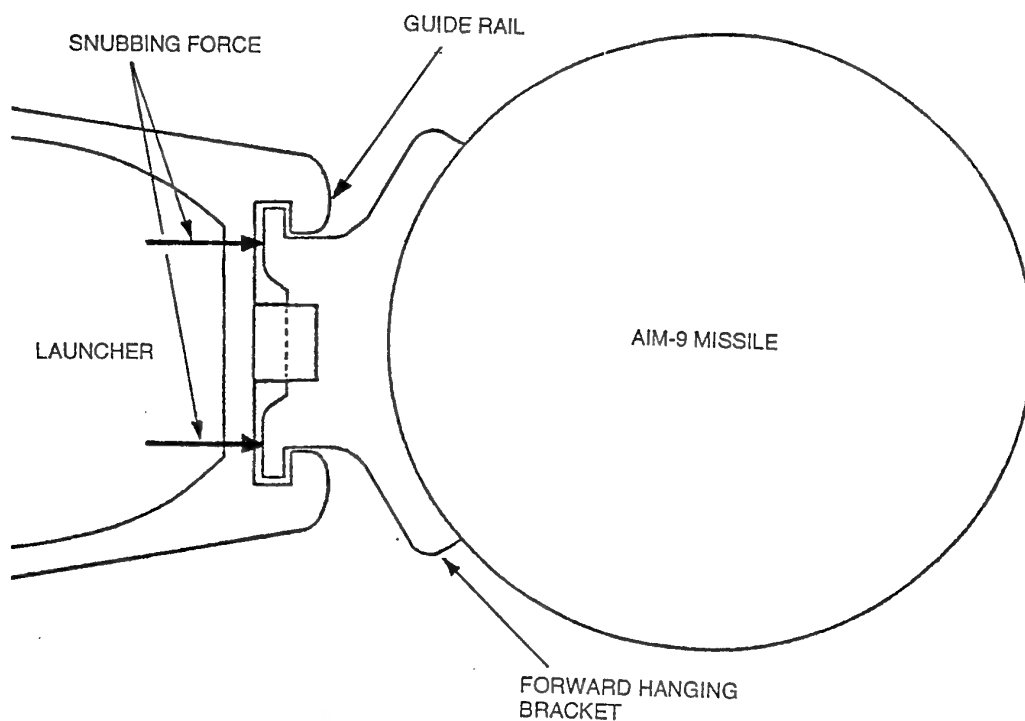


Figure 2. Section through the LAU-7/A launcher guide rail and AIM-9 missile at the location of the forward missile hanging bracket.

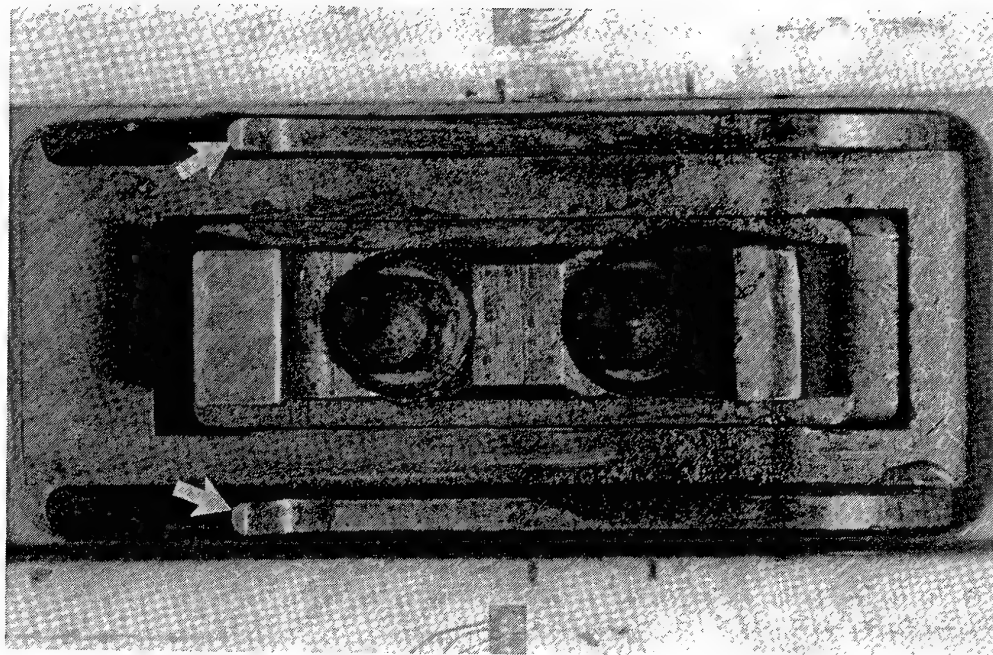


Figure 3. Forward snubber region with forward to the left. The snubber plates (arrowed) are in the engaged position. The hold-back detent mechanism and striker points are visible in the centre.

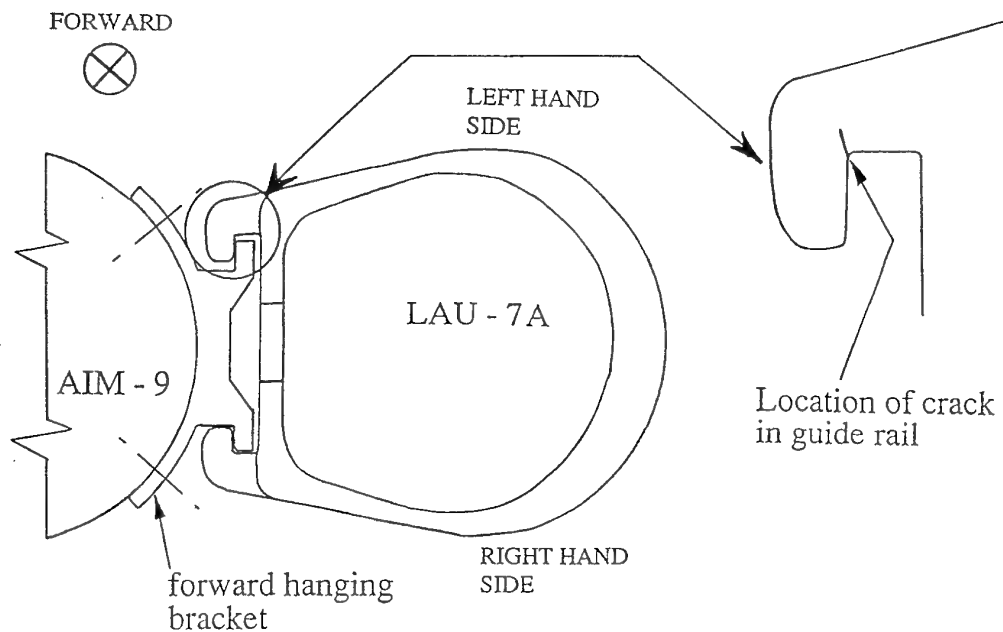


Figure 4. The location of cracking in the LAU-7/A launcher guide rail and typical fatigue crack (inset).

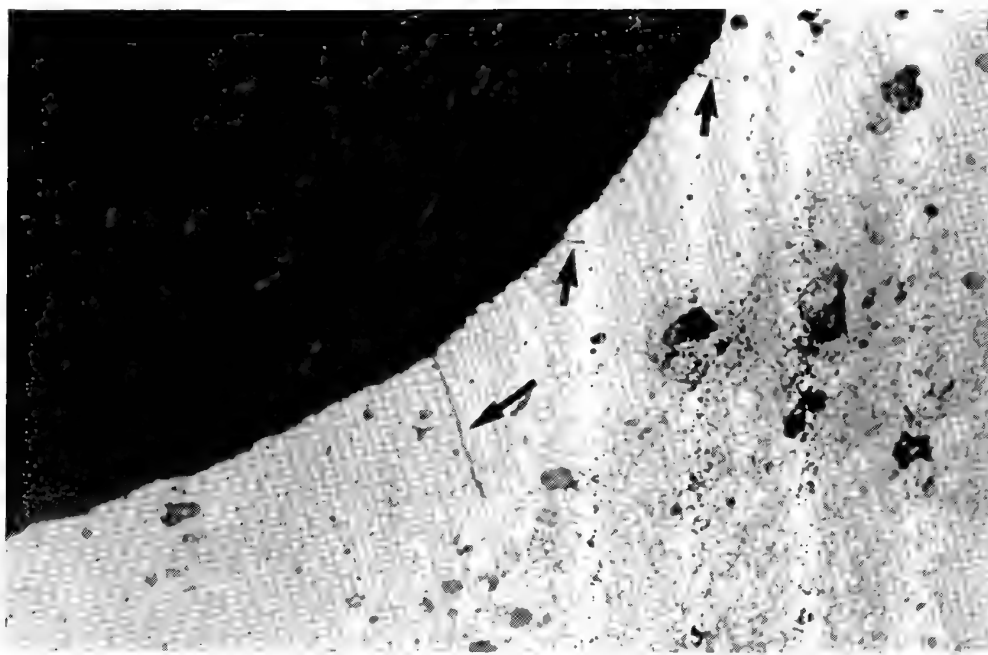


Figure 5. Optical micrograph of the region of cracking in the guide rail of LAU-7/A launcher number 0159, from [2]. 6X

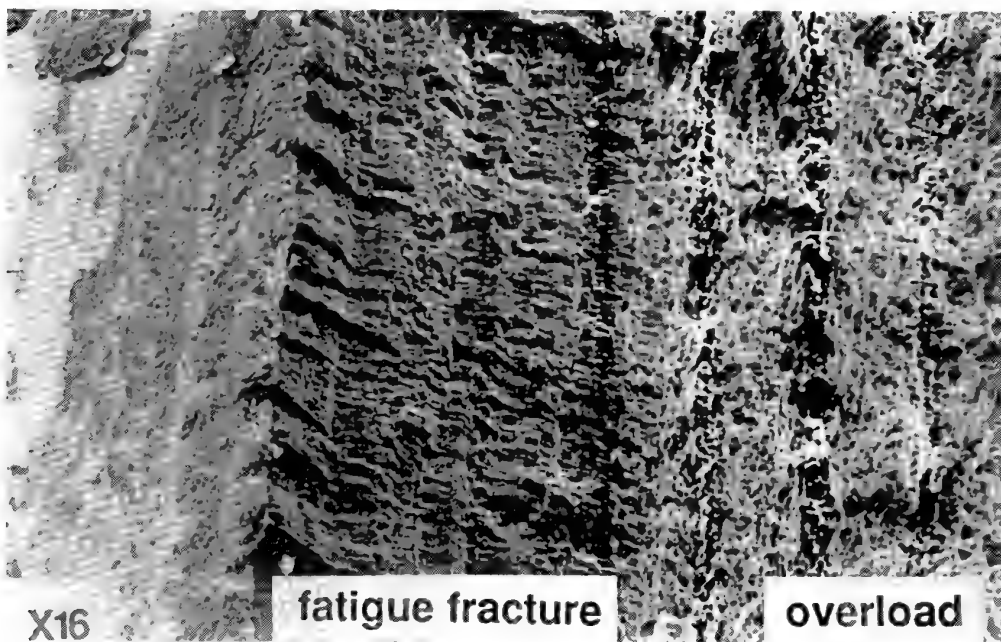


Figure 6. Scanning electron micrograph of the fracture surface from the guide rail of LAU-7/A launcher number 0159, after [2]. 16X

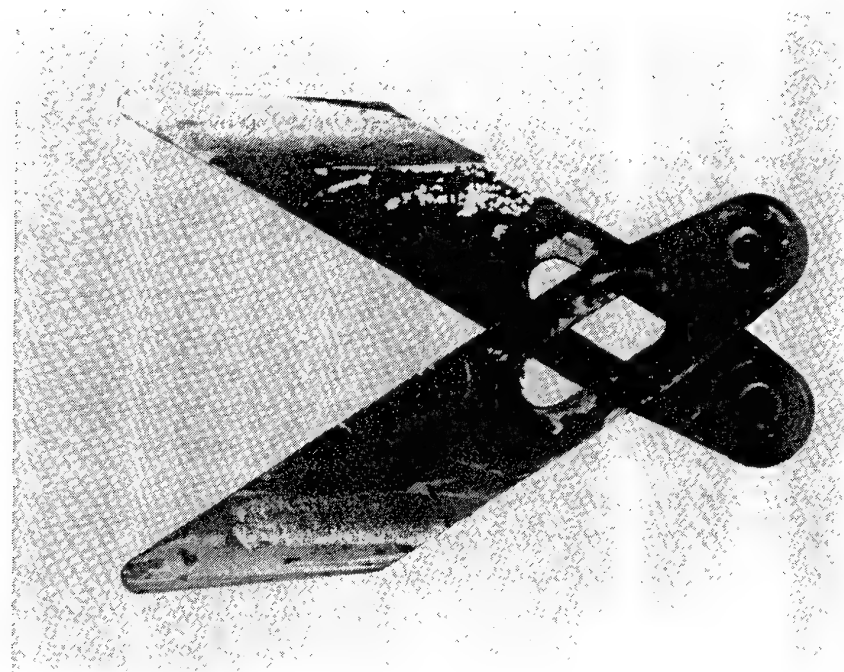


Figure 7. Worn scissor blades from the aft snubber mechanism. Scissors were painted black prior to cycling to illustrate the wear which reduces snubbing effectiveness

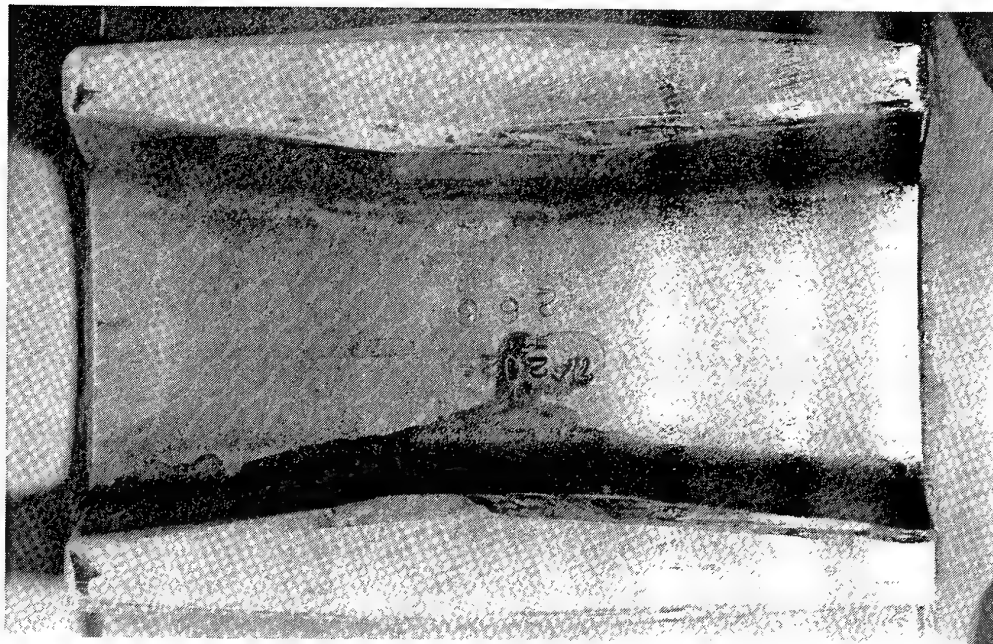


Figure 8. Wear of the inner corners of the aft hanging bracket corresponding to that of the scissors.

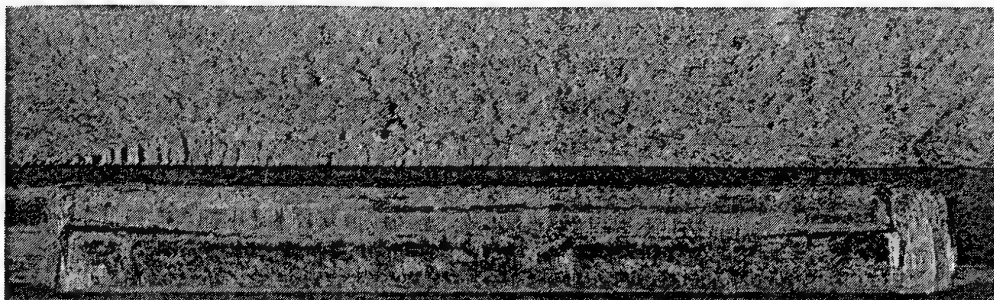


Figure 9. Wear of the inside surface of the rail over the contact zone of the forward hanging bracket. The hills and depressions of the wear marks cause great difficulty for NDI processes. The fatigue crack grown under the test load spectrum is difficult to discern from the overload failure zone.

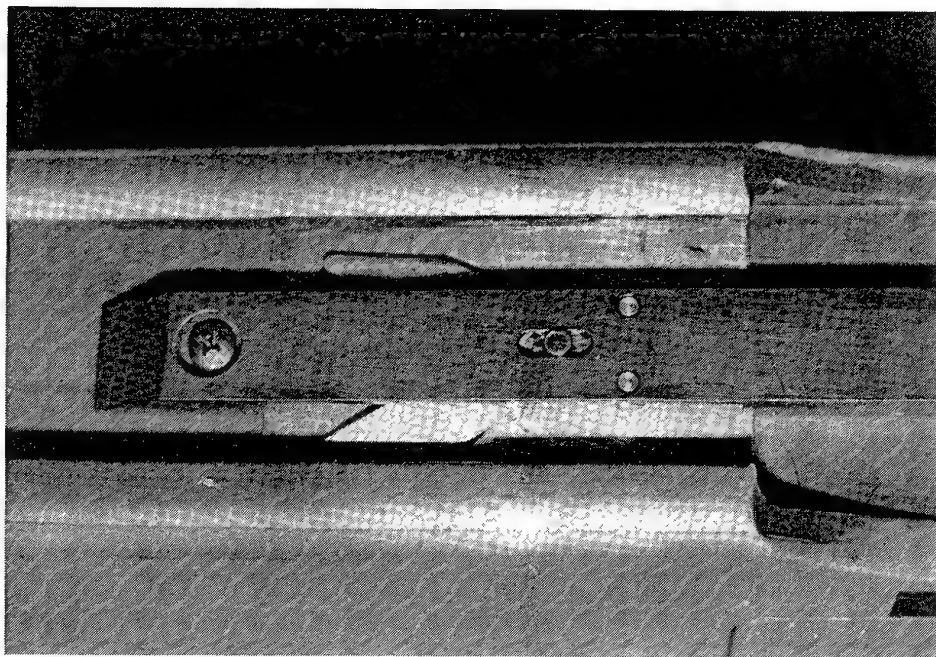


Figure 10. The RAAF wear plate installed under the aft snubbing mechanism in an attempt to force the missile hanger against the rail and restrict vertical movement.

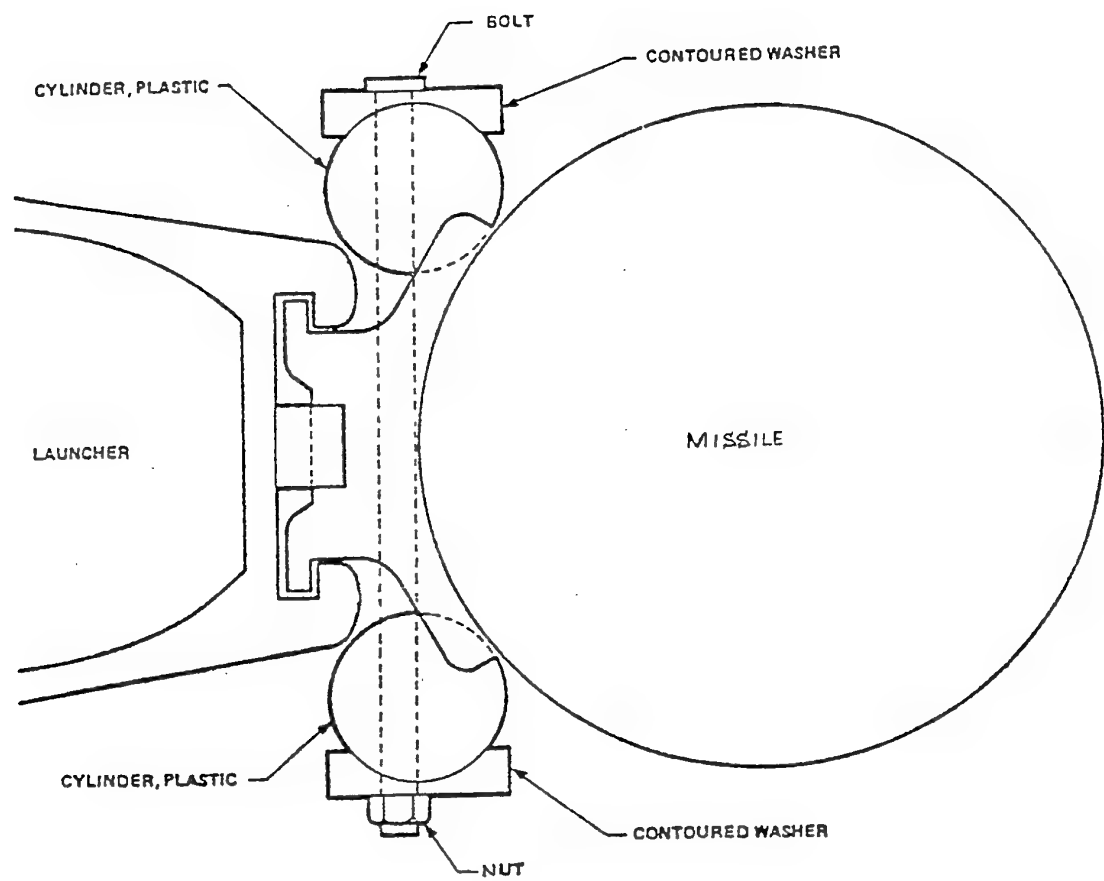


Figure 11. A cross section of the launcher-missile combination showing the CF design of teflon cylinders to increase snubbing forces. The teflon prevents damage to either part, but soon deforms and loses effectiveness.

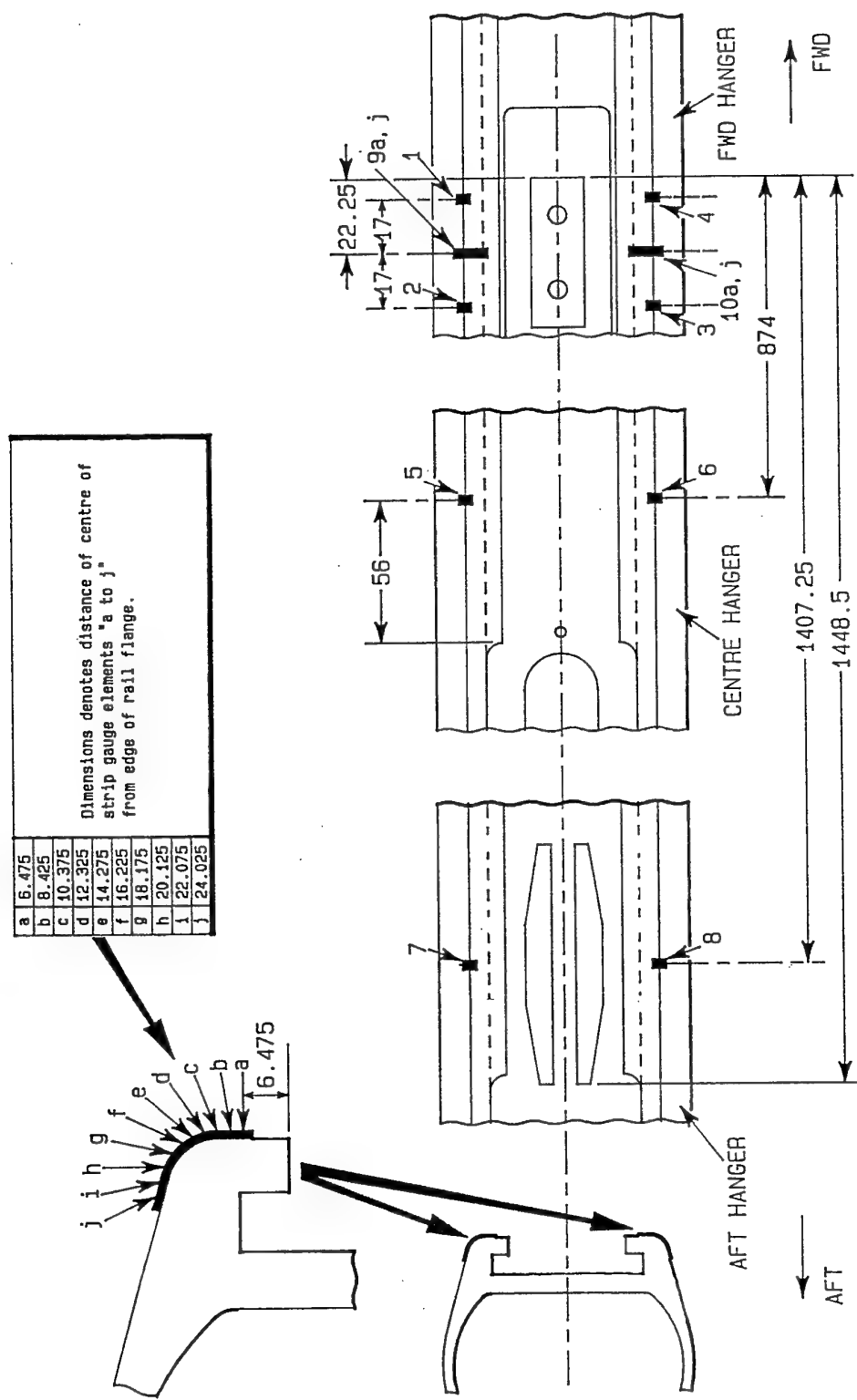


Figure 12. Launcher strain gauge positions

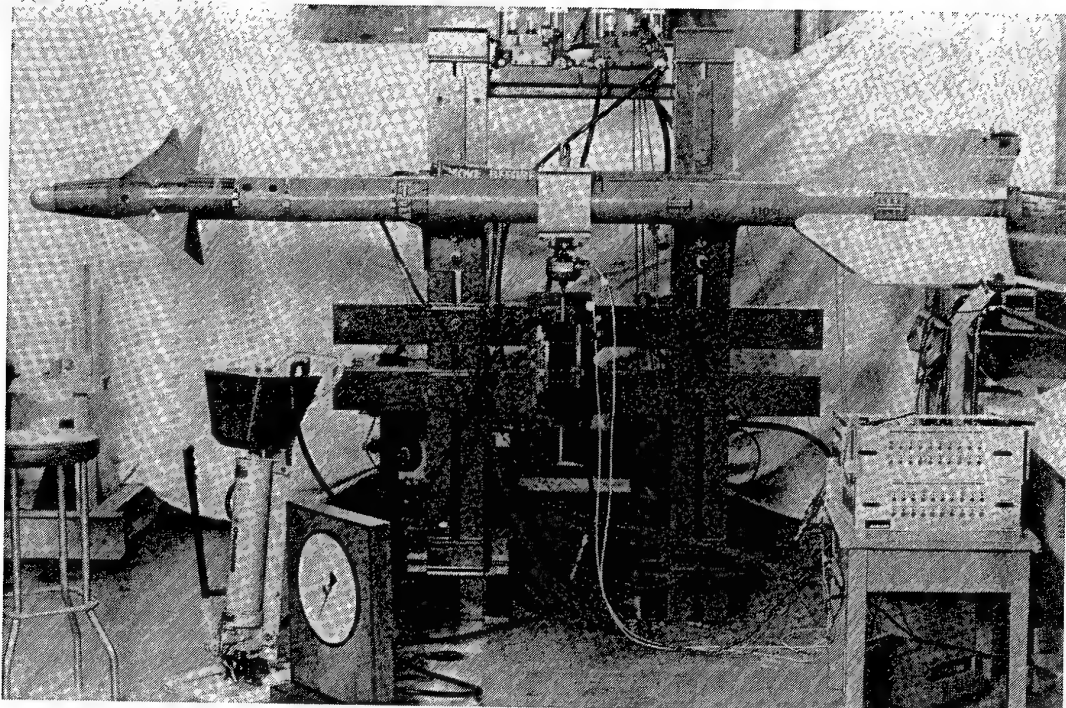


Figure 13. Front view of the test rig with an AIM-9 Sidewinder installed. The hydraulic actuator is connected to the hand pump and pressure gauge as for the static strain surveys.

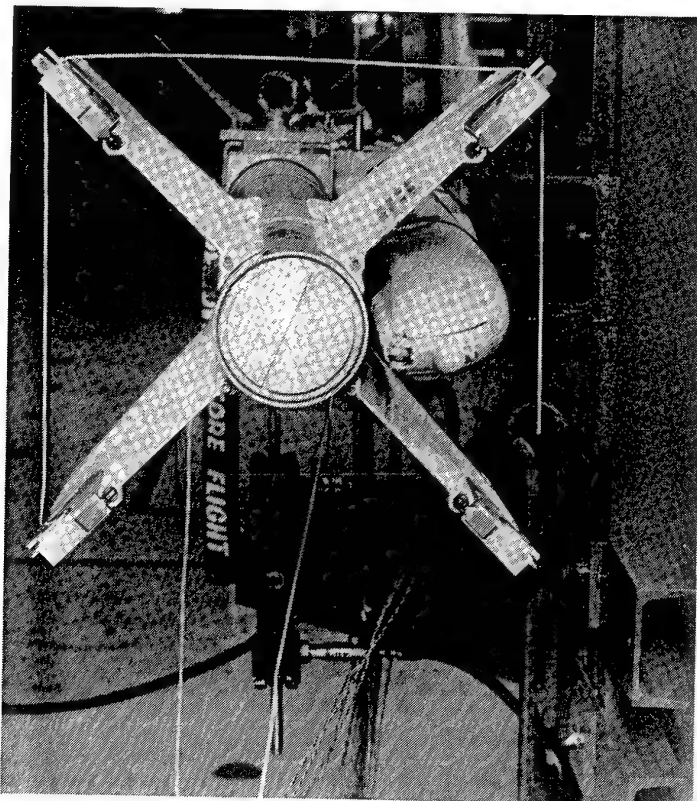


Figure 14. Rear view of the dummy missile and launcher in the rig with the torque strap and dead weight carry attached to the rear fins.

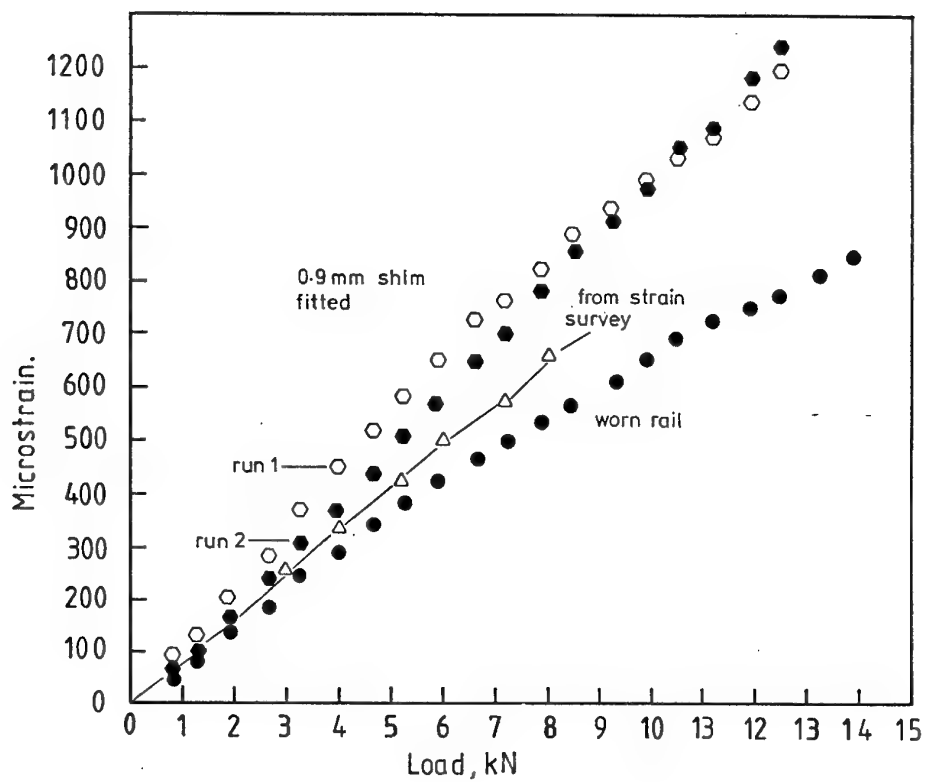


Figure 15. Effect of shimming forward hanging bracket in the guide rails during a fatigue test.

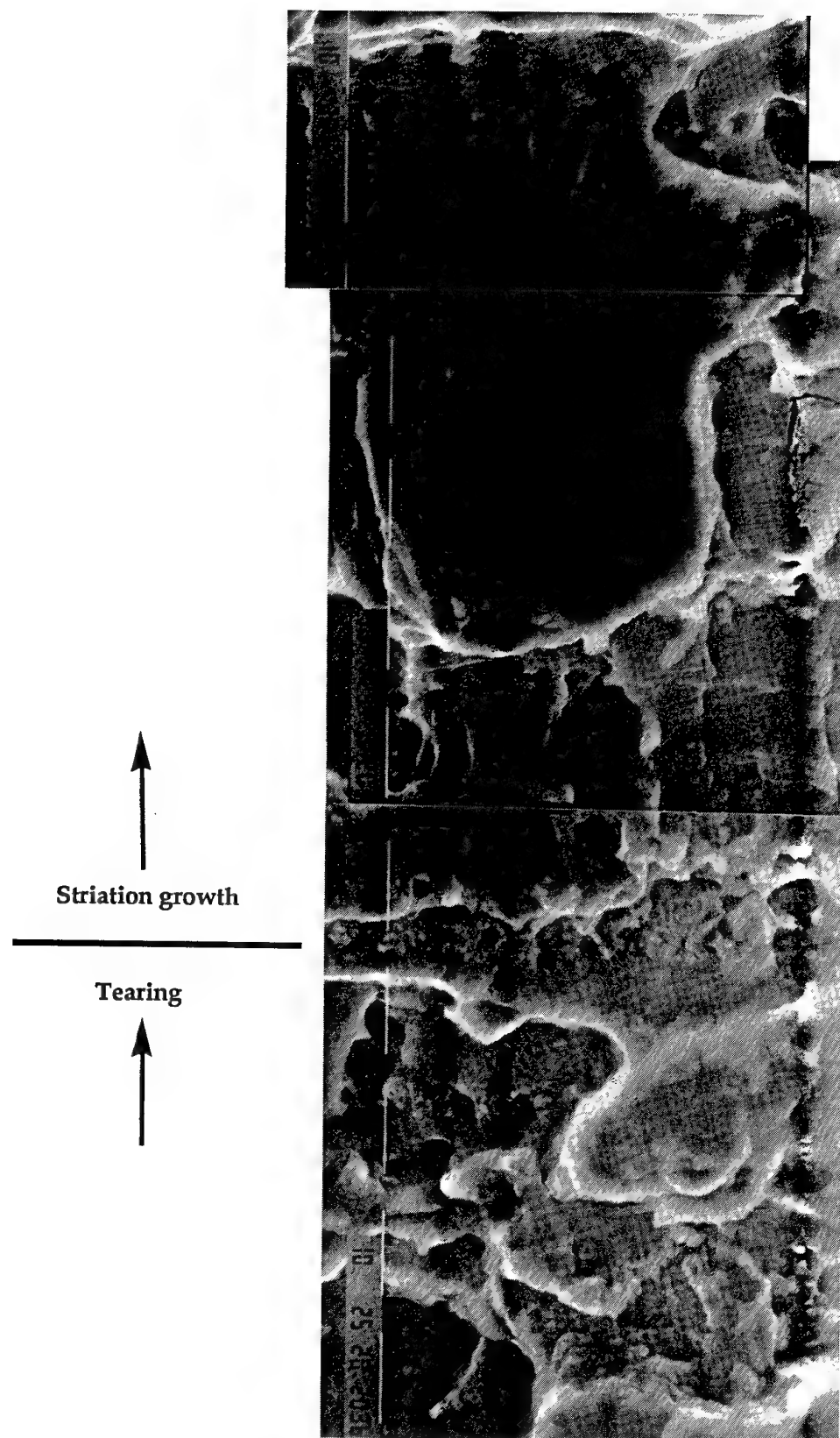


Figure 16. Fatigue crack growth in the guide rail of launcher NMH 0217 due to service loads. Within the striation bands growth occurs at an average of 900 striations per mm.

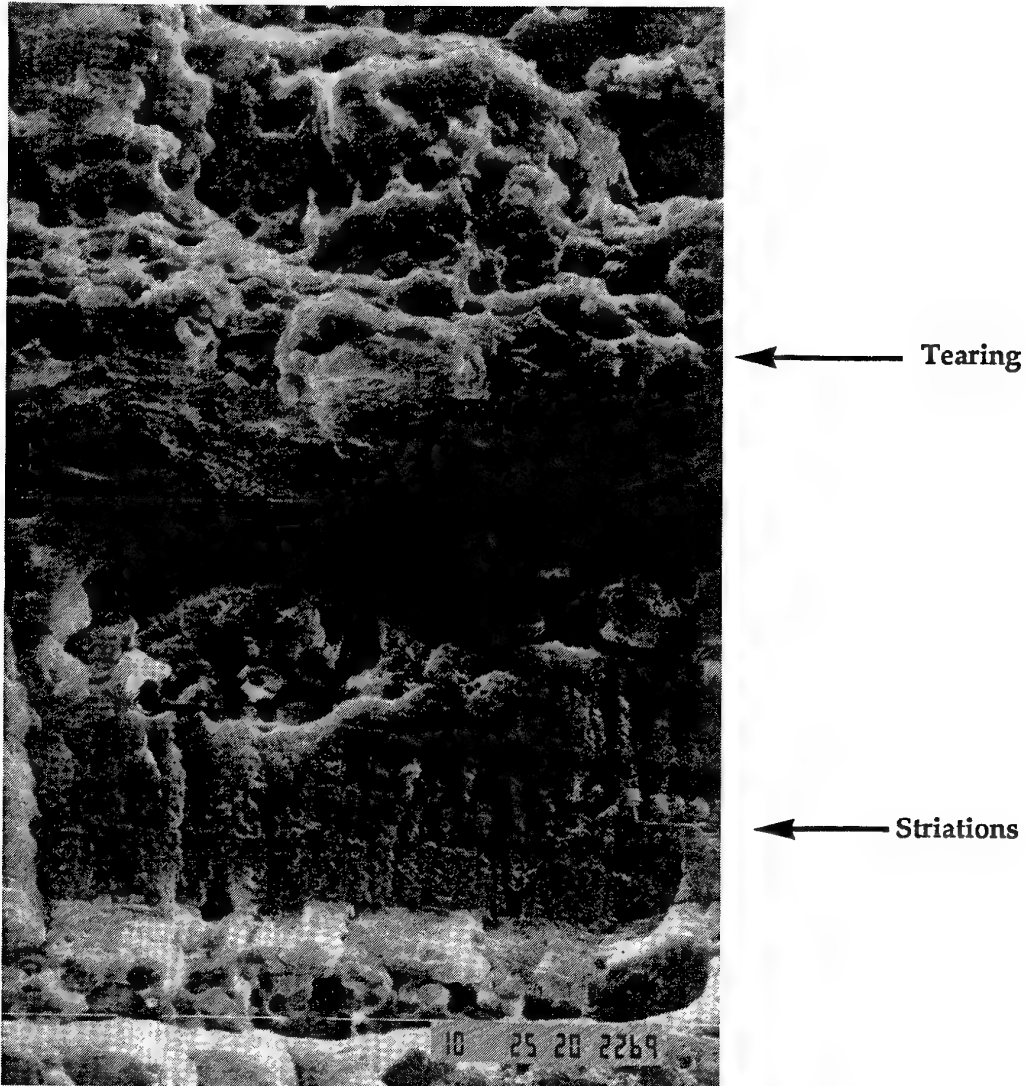


Figure 17. Another example, from a launcher found overloaded in operational service, of fatigue crack growth interspersed with ductile tearing . This scanning electron micrograph is of launcher S/N 0355.

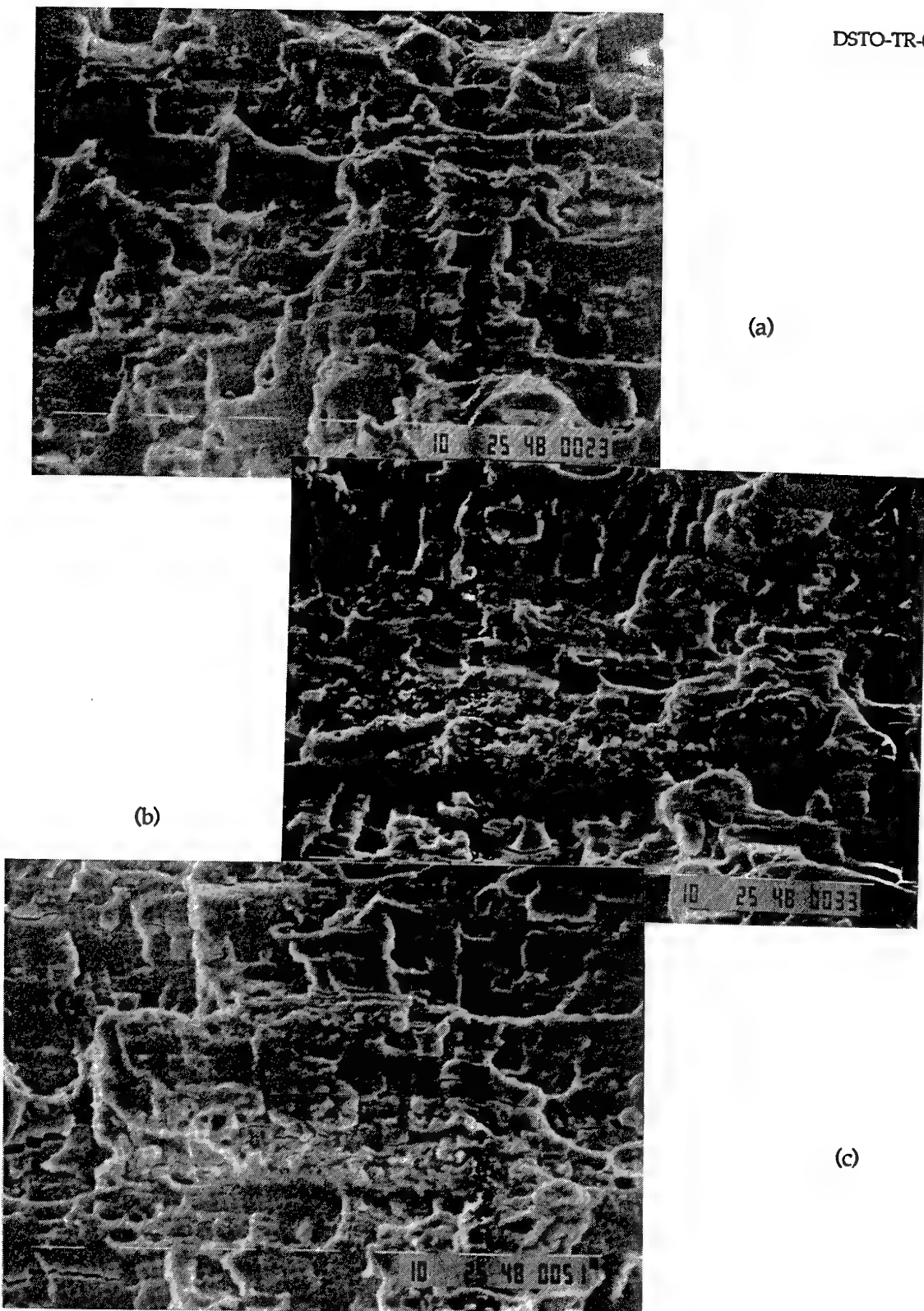


Figure 18. Fatigue crack growth in guide rails of launcher 71032-012 tested in the laboratory. (a) initial cracking in service, (b) Nz spectrum factored by 3.0, (c) final stages of cracking with spectrum factored by 2.5

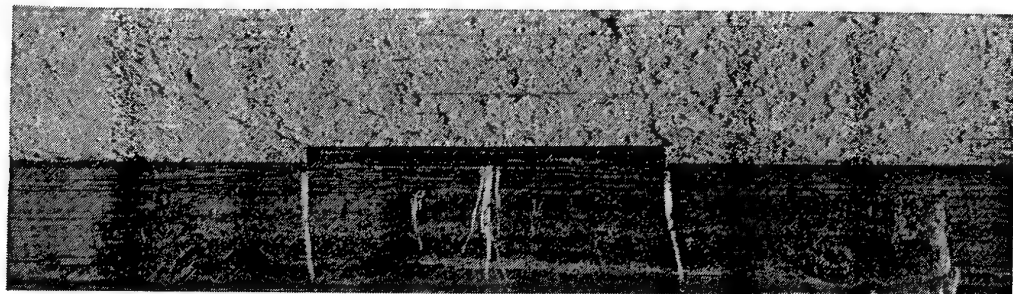


Figure 19. Fatigue crack growth from an EDM notch in the guide rail (inset) of launcher 0175. The delineation between the melted grains of the notch and the sharp edges of the striation crack growth is difficult to discern.

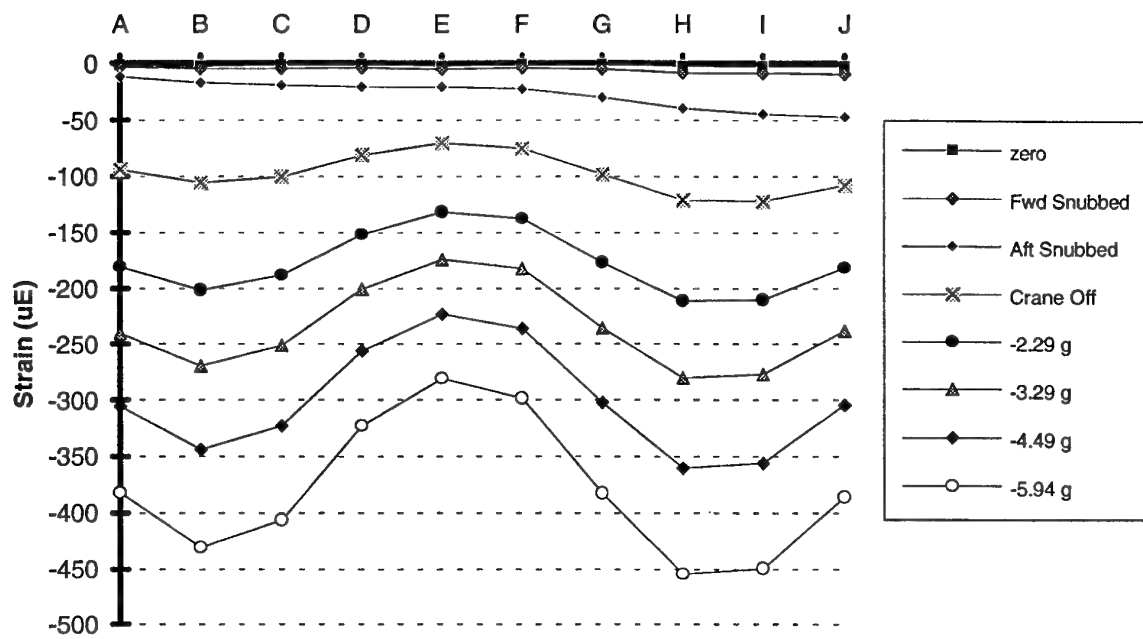


Figure 20. Strain results from the strip gauge on the upper rail during snubbing and subsequent down loading to 5.95g (Experiment 7). The two peaks at gauges B and H lie either side of the line of extension of the crack.

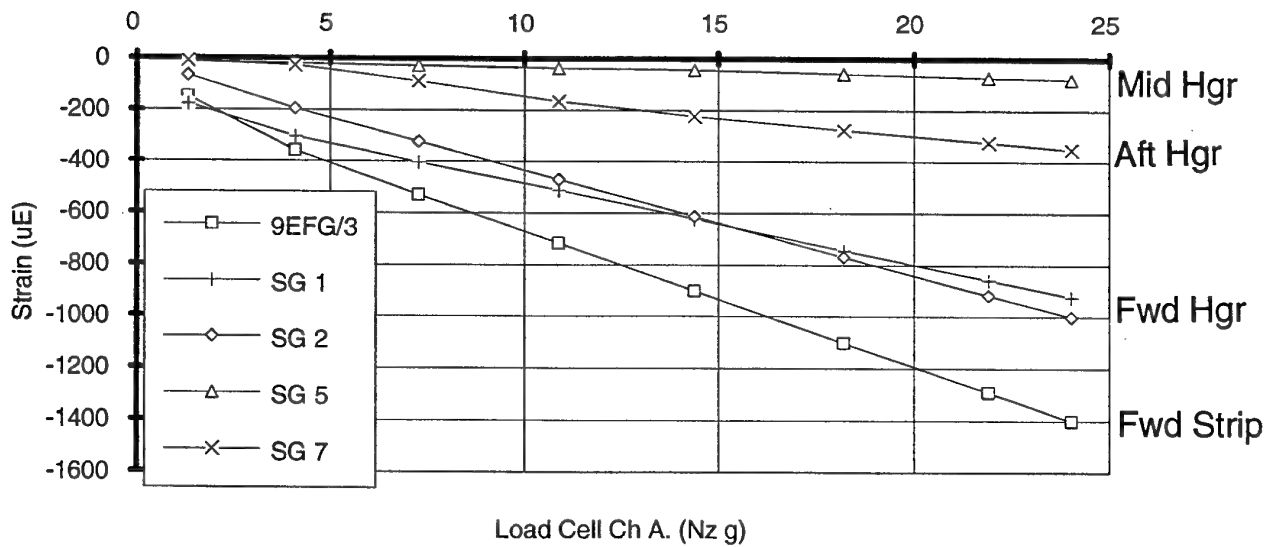


Figure 21. "Load shedding" as seen by comparing the strip gauges (average of E, F and G) at the forward hanger with the single gauges at the mid and aft hangers. These strains are from the loaded rail in Experiment 27.

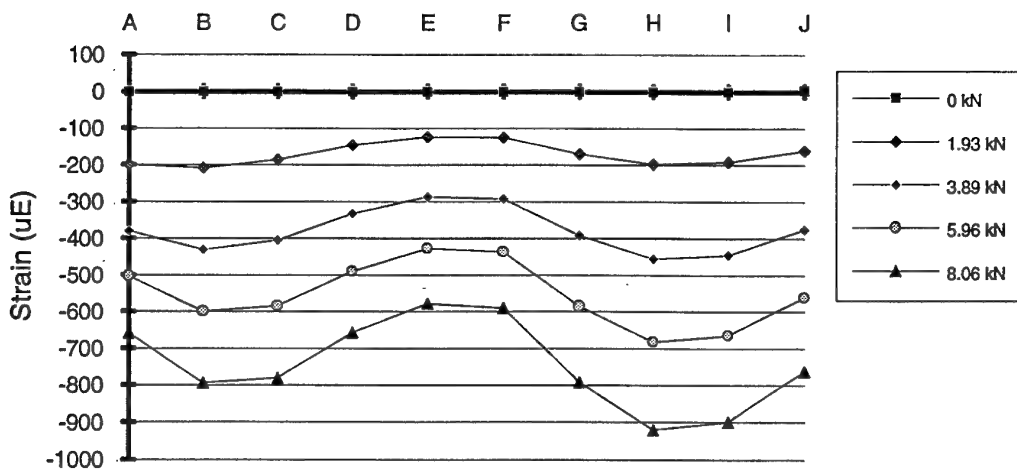


Figure 22 (a). The effect of the crack on strains in the guide rail : Strip gauge strains at the forward snubber on the cracked lower rail during 8.5g up loading of Experiment 5.

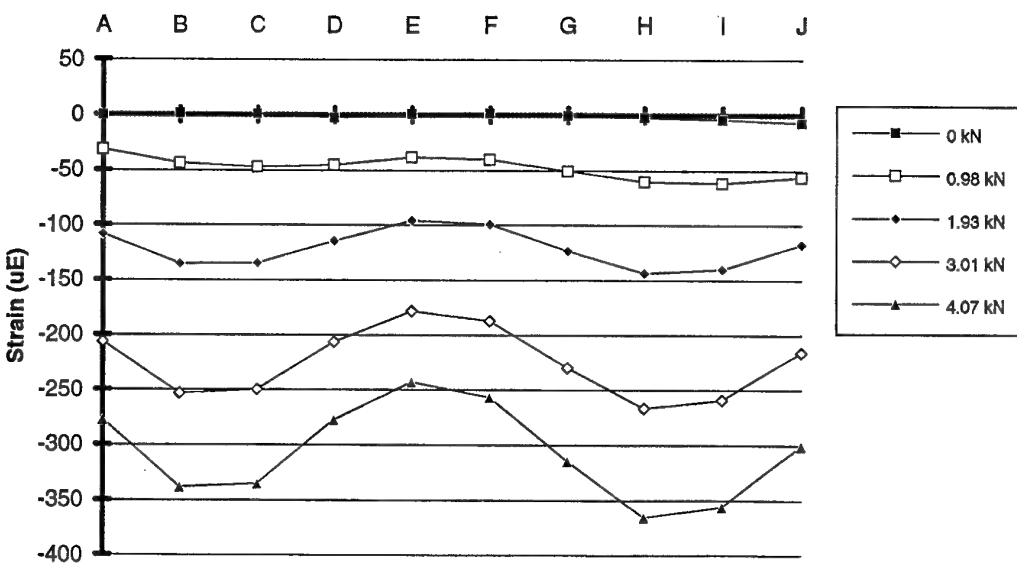


Figure 22 (b). The effect of the crack on strains in the guide rail : uncracked lower rail during up load of Experiment 20.

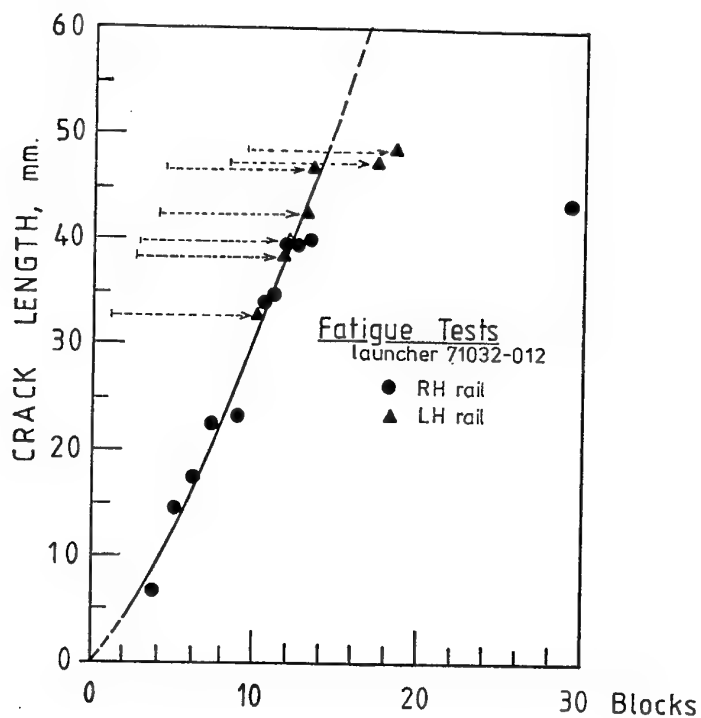


Figure 23. Crack growth in the guide rails of launcher 0148 from laboratory fatigue test.

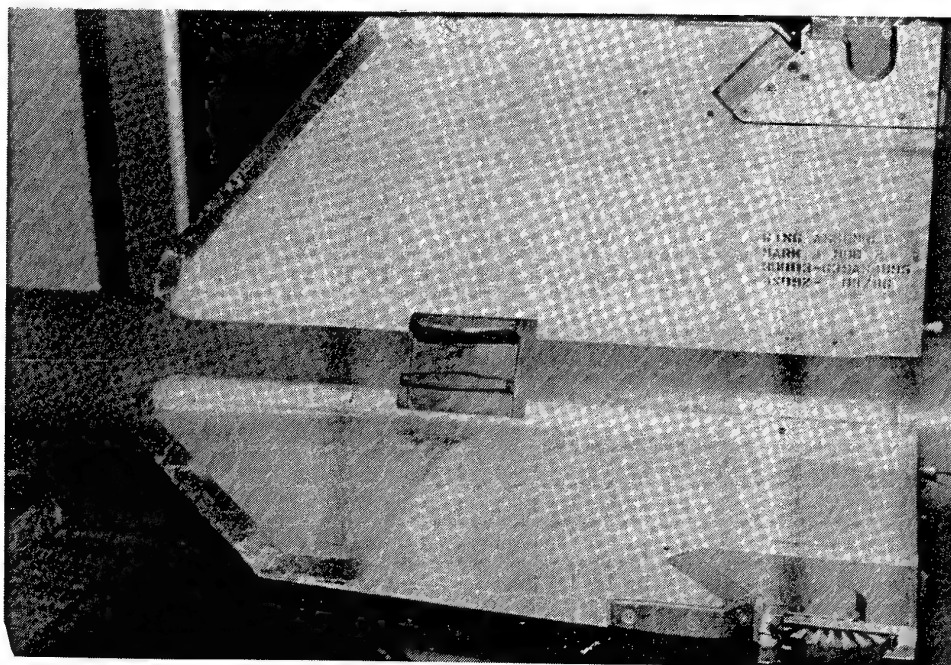


Figure 24. Dark debris particles deposited on the fin as a result of wear at the aft hanging bracket during fatigue testing.

APPENDIX A

Loading Evaluation and Fatigue Test Spectrum Development

A1. Choice of Spectrum

The loading on the LAU-7/A consists of loads from the missile (AIM-9 Sidewinder) and reactions through the two wing attachment bolts. The loads on the missile arise from 5 major sources.

A1.1 Inertial Manoeuvre Loads

Accelerations at the rigid body aircraft centre of gravity (C-of-G) are significant. The two dominant load cases are normal (N_z) acceleration and roll acceleration (Ω). Preliminary calculations indicated that Ω is not as severe as N_z . The accelerometer data shown in table A1.1 indicates lesser vertical accelerations at the hanging brackets (accelerometers 2 and 4) for 1g rolls than maximum g wind-up-turns. Rolling at constant velocity also places an equal shared outboard load on both upper and lower rails. Also, the combination of rolling and pitch-up was possibly not fatigue significant because the roll rate is very slow at high g levels due to the F/A-18 Flight Management Computer roll limiting schedule [1]. Possibly the next most significant loads after N_z at the C-of-G are the normal loads due to roll acceleration rather than the lateral loads due to roll rate.

A1.2 Aerodynamic Manoeuvre Loads

The complex flow field around the F/A-18 wing tip is not amenable to accurate calculation of the lift generated by the missile body and aft fins/wings. When estimating the fin maximum airloads two contradictory factors must be considered. The lift induced vorticity at the wing tip is strongest at low speed and high alpha and this gives the highest local angle of attack for the fins, resulting in the highest fin lift coefficient. However, the velocity is a squared term in the simple Bernoulli lift equation and so fin lift will increase with airspeed even though the lift coefficient decreases.

Using conservative assumptions, such as angle of attack at 10° on each aft fin and an airspeed of 600 kn, preliminary calculations of the aerodynamic loads were made.

Using these loads as a basis, simulated aerodynamic torsion loads were applied to the aft fins of the AIM-9 and the strains recorded at each hanger location on the launcher rail. These experiments showed that the strains caused by the calculated aerodynamic loads may be greater than the strains caused by vertical inertia loads (N_z loads) through the missile centre of gravity. The "factoring" of loads may overcome this limitation to some extent. However, the difficulty in development and applying an aerodynamic load spectrum places overall limitations on application of this loading type. The simple calculations resulting in the above conclusions are presented below with the gross assumptions and calculated values preceding.

$$\alpha = 10^\circ = 0.175^\circ \quad \text{Span Efficiency Factor, } e = 0.5$$

$$C_L = 2\pi\alpha = 1.1 \quad \text{Radius of action of lift forces, } r = 3.14\text{in}$$

$$V = 600\text{kn} = 1011\text{ft/s}$$

$$\rho = 0.00238\text{slug/ft}^3$$

$$S = 0.93\text{ft}^2$$

$$\text{Aspect Ratio, } A = 2$$

$$L = \text{lift of one fin due to the tip vortex}$$

$$= e\rho V^2 S C_L / 2$$

$$= 622 \text{ lb}$$

Then,

$$T = \text{torque on missile due to 4 fins}$$

$$= 4 L r$$

$$= 7807\text{inlb}$$

In an attempt to estimate the maximum possible torque generated by aerodynamic loading another calculation was performed using Mach = 1.3 and $C_L = 0.5$ for the consequent lower angle of attack. The maximum torque is double the value calculated for the 600kn case above.

A1.3 Wing Vibration Loads

The F/A-18 wing has stable oscillation modes within the flight envelope. These modes change with the carriage of the AIM-9 and other stores. An environmental program to examine the vibration environment of the LAU-7/A launcher has been undertaken at Pacific Missile Test Center, (PMTC) [2]. This stemmed from observed failures of the LAU-7/A system in U.S. Navy service. Some of these failures, or deficiencies, included missing blast shields, loose nitrogen receivers, broken snubber fittings and jammed snubbers. However, no fatigue failures of the guide rails were reported. Instrumented launchers gave vibration accelerations as high as 50g in both the vertical (z) and lateral (y) directions, but only at or near either end of the launcher.

The PMTC report [2] shows that under certain manoeuvres and flight conditions ("points-in-the-sky") the accelerations in the Y and Z directions are as high as 9g at locations adjacent to the forward hanger bracket. These data are summarised in Table A.1.1. The accelerations at the forward hanging bracket locations (accelerometers 2Z and 2Y in the Table) were found to be significantly lower than at some other locations on the launcher, e.g. the rear fairing. Near the forward hanging bracket it appears that the vibrational loads are of the same order as the N_z manoeuvre loads. High energy levels were found below 10Hz, and this was believed to be the cause of the failures of the missile hanging bracket.

Additional data on the loads seen by the AIM-9 missile can be gained from Ref. [3]. The work showed that the accelerations measured on the LAU-7/A launcher during flight trials were higher than those derived through MIL-A-8591G [4], see Table A1.2 [5]⁸ and Figure A1.1. The particular concern, here, was the high accelerations generated by the release of MK 84 bombs (up to 32.7 g) although this was lower than that calculated by MCAIR (50 g).

Whilst accelerations in the launcher do not translate directly to accelerations of the AIM-9 and then to hanger loads, the implications are that vibration loads may play a part in the fatigue cracking process, particularly those below 10 Hz [2]. The present limitations of the type of equipment available means that there is no cost effective way of applying such loading. Ref. [5] provided a table of flight measured hanger reactions, seen in Table A1.3, which also indicated that the Mk 84 ejection provided the highest forward hanger reaction loads.

A1.4 Gust Aerodynamic Loads

Gust loading on the missile cannot use simple models such as a 25 feet/second design limit gust as in the design codes. Again, as with steady aerodynamic loading, the air flow field is complex.

A1.5 Dynamic Manoeuvre Transient Loads

When the controls of the F/A-18 are deflected sharply there are possibly unexpected transient loads applied at the wing tip due to the flexibility of the wing structure. In other words, the inertia loads at the tip are not always closely correlated with the N_z acceleration of the aircraft C-of-G. These can, to some extent, be accounted for by factoring the N_z load spectrum.

A1.6 Summary

The possibilities of undertaking flight trials to measure loads and accelerations on the LAU-7/A launcher were investigated early in the experimental program, but this was found to be not possible in the short term.

⁸Some of the work reported in Ref. [5] was undertaken by Naval Weapons Center (NWC).

Since an N_Z spectrum from a service aircraft was available, covering the period of RAAF flying which produced the cracking in the launchers it was decided to use this as the basis for the test program. It was considered appropriate to "factor up" the N_Z spectrum and base the assessment of the spectrum on a comparison of fatigue fracture surfaces from service failures and tests and also fatigue-life behaviours.

A2. Fatigue Test Spectrum Development

As result of the considerations above and the available test equipment, the spectrum applied was an Inertial Manoeuvre Load spectrum, as mentioned in Section A1.1. The spectrum consisted of turning points which were peak-valley values collected by the MSDRS system on F/A-18 A21-015 from the vertical direction accelerometer located near the aircraft centre of gravity. In the MSDRS files they are identified as code 49/50 data. The period covered by these data was January to August 1987 for No. 3 Squadron, RAAF Williamtown. For the period covered by the data used in the generation of the spectrum it is known that aircraft A21-015 was involved in air-to-air combat training and this resulted in flying in a manner which resulted in a more severe g-exceedance spectrum than US Navy or McDonnell spectra [5, 6, 7]. Air-to-air combat training involves carriage of either AIM-9 dummy air training missles (DATM) or completely inactive AIM-9 missles. LAU-7/A launcher S/N 0217, exclusively carried on aircraft A21-015, was found to have cracked in 234 hours of flying. This is the shortest fatigue-life exhibited by the failures in the RAAF stock of launchers.

The fatigue test spectrum was generated by combining the data of files from 5 tapes of MSDRS data: M1168; M1169; M1174; M1162 and M0263. The combined spectrum contains 6426 turning points with max value of +8.07 g and minimum value of -1.74 g. These are normal acceleration g values. This spectrum represents 191.8 hours of aircraft flight time. The files, as supplied, had been checked for non peak-valley-peak turning points, however a small program CHECKSEQ.PAS was also used to re-check the sequence in its combined (full length) form.

The combined sequence on the AMRL Elxi computer (LAUSEQ.CHK) was transferred to a VAX computer which then was used to write a file which was used in the AMRL-designed Stand Alone Controller (SAC). For the purposes of machine control the g values derived from the flight data are converted in bit values which correspond to machine voltage levels.

The maximum bits (2047) was set to 9.0 volts for this test program. This is summarised in Table A2.1.

The g values, and hence the bit values, can be converted to Newtons with the mass of the missile:

$$M_m = 86.1 \text{ kg} = \text{mass of AIM-9 missile}$$

$$M_m + M_{lc} = 99.0 \text{ kg} = \text{mass AIM-9 + load carrier}$$

Since an 8.07 g acceleration at the aircraft C of G nominally places the same acceleration on the AIM-9, the load seen by the LAU-7/A is = 6816N (at maximum g).

Since:

$$P_{TOT} = P_{LCR} + P_m + P_{lc}$$

where:

P_{LCR} = load cell reading in Newtons

$$\begin{aligned} P_m + P_{lc} &= \text{weight of missile and load carrier} \\ &= 971\text{N} \end{aligned}$$

using the sign convention that a positive g gives negative (i.e. down) AIM-9 load onto the LAU-7. The load cell reads negative loads in pulling down in the rig as set up at this time.

Hence:

$$P_{LCR} = P_{TOT} - (P_m + P_{lc})$$

Example:

at Maximum Positive g

$$\begin{aligned} P_{TOT} &= 6816\text{N} \\ P_{LCR} &= 6816\text{N} - 971\text{N} \\ &= 5845\text{N} \\ &= 100\% \text{ of the applied static load} \end{aligned}$$

Consequently, an offset resistor must be introduced to the SAC to account for the weight of the missile and load carrier, ($P_m + P_{lc}$).

The negative g loads (up loads) are scaled in the same manner as positive loads and require the same offset.

A2.1 Factoring of N_z Loads

The higher g loads resulting from dynamic effects can be simulated in the inertia loads spectrum by "factoring" the loads. This would tend to move the whole spectrum upwards, but in the absence of any other loading spectrum this would take the peak loads to known higher g levels. The factoring eventually used in the present work was up to 3X the N_z g levels; viz. the peak g level used was 24.2g. This level may still be low when compared to the levels apparently generated by the release of four (4) Mk84 bombs. MCAIR estimations suggest this could be as high as 50g and NWC flight trials measure this at 37g [5].

A3. References

1. Rider, C.K. private communications.
2. US Naval Air Systems Command, " LAU-7/A Launcher Consolidated Environmental Envelope Program." Pacific Missile Test Center, Point Mugu, January 1985.
3. Van Dyken, R.D. and Merritt, R.G. "AIM-9 Wing-Tip Carriage Aboard F/A-18, Flight Test Report Volume 1. Analysis and Assessment." Naval Weapons Center, NWC TM 6108 Vol. 1, 1988.
4. Military Specification, MIL-A-8591G "Airborne Stores, Suspension Equipment and Aircraft-Store Interface (Carriage Phase); General Design Criteria for" 1 Dec 1983.
5. Glasper, D., Rodgers, R., Heilman, R. and Torres, G. "LAU-127/A Integration Feasibility Study, F/A-18 Wing Tip Use of LAU-127/A Launcher." Pacific Missile Test Center, June 1988 (*Limited Release*).
6. Rider, C.K., Higgs, M.G.J. and Sanderson, S. "Investigation of RAAF F/A-18 Service Usage -1986 (U)." Aeronautical Research Laboratory, Aircraft Structures Division Technical Memorandum, ARL-Struct-TM-501, January 1989.
7. Rider, C.K., Higgs, M.G.J. and Sanderson, S. "Trends in RAAF F/A-18 Service Usage No 2 OCU: May 1985 - April 1987 (U)." Aeronautical Research Laboratory, Aircraft Structures Division Technical Memorandum, ARL-STRUC-TM-518, August 1989. (*Limited Release*).

Table A1.1. LAU-7/A Launcher Accelerometer Peak g Data (from Ref. [2]) During Typical Prescribed Manoeuvres

	Right Max Rolls at 1g H/A	Left Max Roll max g H/A	Wind- up turn H/A	Push Over to -2g H/A	Slow to 400K CAS	Max Rolls at 1g L/A	Max Roll max g L/A	Right Max Roll max g L/A	Left Wind- up turn L/A	Push Over to -2g
Accelerometer										
1Z	11.0	20.0	25.0	20.0	17.0	27.0	9.0	7.0	11.0	16.0
1Y	20.0	20.0	21.0	30.0	30.0	50.0	25.0	7.0	10.0	20.0
2Z	2.0	9.0	5.5	7.0	5.0	4.5	2.5	3.5	4.5	5.1
2Y	6.0	10.0	7.0	8.0	6.0	5.0	2.2	3.0	5.0	4.5
2X	1.2	3.9	5.0	2.5	9.5	3.0	1.1	1.5	2.0	4.0
3Z	5.8	10.0	7.0	10.0	7.0	7.0	5.5	5.5	7.0	8.5
3Y	3.9	6.5	5.5	6.5	5.5	4.5	3.1	4.0	5.1	6.5
3X	3.0	5.0	6.0	4.5	4.0	5.0	2.5	4.0	4.0	6.0
4Z	3.0	7.0	7.5	9.0	3.5	6.5	3.0	5.0	5.5	7.0
4Y	7.5	11.0	12.0	15.0	6.5	10.5	8.5	9.0	10.0	15.0
4X	3.8	8.5	8.0	9.5	3.5	7.5	3.5	7.0	6.5	7.0
5Z	3.5	7.0	8.0	10.5	4.5	5.9	3.0	3.1	4.0	5.0
5Y	7.0	18.0	19.0	20.0	7.0	10.0	7.0	10.5	11.0	12.0
5X	3.8	8.0	9.5	6.5	6.0	4.0	2.0	3.0	4.0	5.0
6Z	20.0	45.0	40.0	45.0	30.0	50.0	17.0	40.0	35.0	40.0
										25.0

**Table A1.2. AIM-9 Captive Carriage Translational and Rotational Peak Accelerations.
(from Ref. [5])**

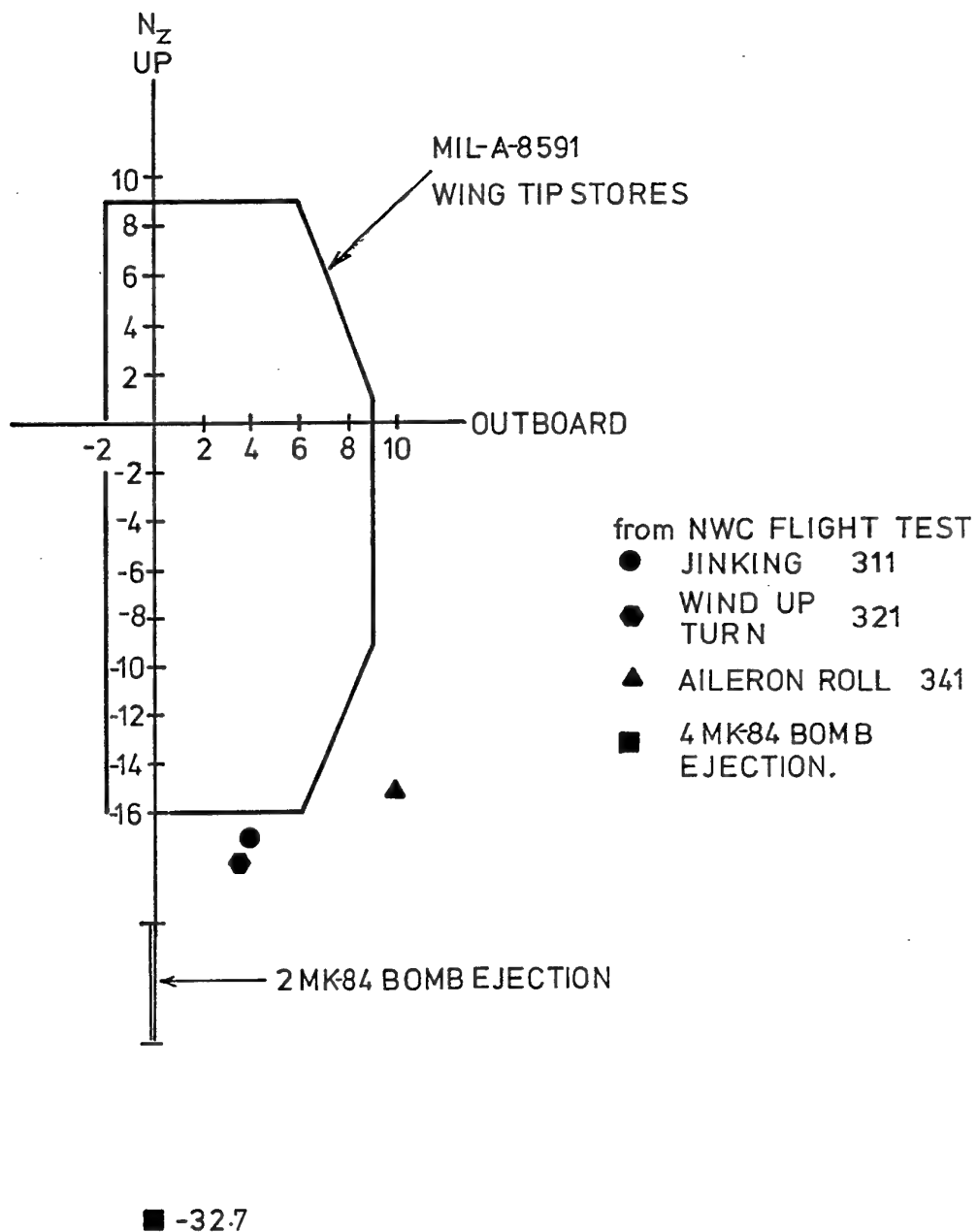
Load Case	Event or Manoeuvre	Source	a_x	a_v	a_z	Ω_x	Ω_v	Ω_z
			g	g	g	rad/sec ²	rad/sec ²	rad/sec ²
111	CFL-2	MIL-A-8591G	-1.5	-6.0	15.5	0.0	4.0	-2.0
112		Proc A	-1.5	6.0	15.5	0.0	-4.0	-2.0
121	CFL-6		-1.5	-9.0	9.0	0.0	4.0	-2.0
122			-1.5	9.0	9.0	0.0	4.0	-2.0
131	AL-2		3.0	-5.0	12.0	-100.0	25.0	6.0
132			3.0	5.0	12.0	-100.0	25.0	6.0
141	AL-6		9.0	-2.5	5.0	-100.0	25.0	6.0
151	CAT-1		9.0	-2.5	5.0	-25.0	15.0	4.0
211	Pullout	MIL-A-8591G	-1.5	-1.0	10.4	-0.5	-0.5	0.0
212		Proc B	-1.5	1.0	10.4	-0.5	-0.5	0.0
221	Rolling		-2.8	15.2	16.6	-17.0	-3.0	-2.0
222	Pullout		-0.4	15.9	16.6	-17.0	-3.0	2.0
231	Barrier		1.5	-1.7	3.0	0.0	-6.0	-4.0
232	Engagement		6.1	1.7	3.0	0.0	-6.0	4.0
241	MAX SNK-RT		-0.3	-1.3	4.7	0.0	-4.0	-2.0
242	Landing		2.0	1.3	4.7	0.0	-4.0	2.0
251	BNK-to-BNK		-2.1	-0.8	13.6	-13.0	-0.5	-1.0
252	Roll		-2.1	1.2	13.6	-13.0	-0.5	-1.0
261	RDDR-Kick		-2.4	-1.7	1.6	-1.0	0.0	-1.5
262	Release		-2.4	1.3	1.6	-1.0	0.0	-1.5
271	Pushover		-1.5	-1.0	-6.3	0.5	0.0	0.0
272			-1.5	1.0	-6.3	0.5	0.0	0.0
311	Jinking	NWC	-1.5	-4.0	17.0	0.0	-42.0	-16.0
312		FLIGHT	-1.5	-4.0	17.0	0.0	42.0	-16.0
321	Wind-Up	TEST	-1.5	-3.0	13.0	0.0	-62.0	-26.0
322	Turn	DATA	-1.5	-3.0	18.0	0.0	62.0	-26.0
331	Symmetric		-1.5	-3.0	16.0	0.0	-44.0	-26.0
332	Pull-up		-1.5	-3.0	16.0	0.0	44.0	-26.0
341	Aileron		-1.5	-10.0	15.0	0.0	-15.0	-4.0
342	Roll		-1.5	-10.0	15.0	0.0	15.0	-4.0
351	Asymmetric		-1.5	-2.0	9.0	0.0	-70.0	-33.0
352	Roll		-1.5	-2.0	9.0	0.0	70.0	-33.0
361	Arrested		4.0	-3.5	12.5	-100.0	-60.0	-45.0
362	Landing		4.0	-3.5	12.5	-100.0	60.0	-45.0
411	MK 84	MCAIR	-1.5	0.0	50.0	0.0	0.0	0.0
511	Bomb	NWC	-1.5	-3.0	32.7	0.0	-66.0	-38.0
512	Ejection	FLIGHT	-1.5	-3.0	32.7	0.0	66.0	-38.0
513		TEST	-1.5	3.0	32.7	0.0	-66.0	-38.0
514		DATA	-1.5	3.0	32.7	0.0	66.0	-38.0

**Table A1.3. Reactions at Hangers for Captive Carriage Load Cases (Limit Loads).
(from Ref. [5])**

Load Case	R _{fx} lb	R <subfy< sub=""> lb</subfy<>	R <sub fz<="" sub=""> lb</sub>	M _{fx} inlb	R _{mv} lb	R _{mz} lb	M _{mx} inlb	R _{av} lb	R _{az} lb	M _{ax} inlb
111	292	1881	555	-4979	-1177	5B3	-10353	-2041	1371	-13673
112	292	1881	-944	-4982	-1177	423	-10354	-2041	749	-13669
121	292	1892	845	-11670	-2690	816	-21650	-3487	2041	-25443
122	292	1892	-1404	-11673	-2690	577	-21650	-3487	1125	-25451
131	-591	1948	784	4043	393	-74	3700	373	243	877
132	-591	1948	-463	4044	393	-207	3700	373	-266	878
141	-1725	1177	608	2129	69	-259	1850	145	133	437
151	1685	840	175	1611	108	218	1447	121	84	339
211	284	1252	-38	-6400	-1371	496	-11697	-2176	1095	-13984
212	284	1252	-288	-6398	-1371	468	-11696	-2176	1006	-13984
221	537	2667	-2205	-9530	-2258	527	-19543	-3189	805	-24954
222	68	2667	-2179	-9526	-2258	414	-19544	-3189	756	-24942
231	-267	489	183	1396	273	27	1345	203	105	330
232	-1169	489	-14	1396	273	-221	1345	203	-81	329
241	65	708	124	1874	332	46	1793	253	72	436
242	-386	708	-87	1874	332	-89	1793	253	-67	436
251	401	1635	-92	-5446	-1211	518	-10781	-2071	1088	-13774
252	401	1635	-343	-5447	-1211	491	-10782	-2071	991	-13782
261	460	179	136	444	75	100	428	52	85	102
262	460	179	-239	444	75	60	428	52	-68	102
271	284	-585	-38	-10974	-2146	495	-16115	-2712	1095	-15045
272	284	-585	-288	-10973	-2146	468	-16115	-2712	1002	-15049
311	349	1360	85	-4842	-667	706	-9924	-1818	1311	-13555
312	349	2615	86	-4342	-1471	707	-9986	-2146	1311	-13605
321	389	1170	-197	-4685	-428	801	-9644	-1699	1296	-13471
322	389	3025	197	-3949	-1617	801	-9737	-2205	1296	-13555
331	389	1218	197	-5127	-693	801	-10187	-1833	1296	-13605
332	389	2533	197	4605	1539	799	10252	2176	1296	-13673
341	300	2269	939	-10141	-2228	851	-20052	-3189	2086	-25055
342	300	2719	939	-9962	-2511	853	-20075	-3338	2086	-25089
351	418	782	-518	-12111	-1974	1054	-21591	-3189	1788	-25426
352	418	2883	-516	-11280	-3316	1055	-21699	-3755	1788	-25493
361	-573	730	-182	3677	1229	427	3895	730	350	968
362	-573	2526	-181	4388	81	427	3805	248	350	884
411	284	5513	-33	13688	2317	39	13214	1609	-5	3148
511	438	2623	-255	8560	2146	484	8689	1326	285	2103
512	438	4604	-257	9345	883	485	8591	797	287	2016
513	438	2623	-1007	8561	2146	405	8691	1326	-20	2103
514	488	4604	-1006	9345	883	406	8592	797	-20	2014

Table A2.1. Correspondence between LAUSEQ and Flight loads.

Bits on Disk	Fatigue Flight Loads (g)
+2047	+8.06
0	0
-2047	-8.06

Figure A1.1 *Flight measured launcher accelerations. [5]*

APPENDIX B

NDI of LAU7/A Launcher Guide Rails

B1. Comparison of Inspection Techniques

The launcher guide rails were inspected using several methods of NDI. Initially the guide rails were inspected at RAAF 481 Wing (Williamtown) using an eddy-current method developed by NDISL (Amberley) [1]. This inspection method was applied to all LAU7A launcher housings which were undergoing routine servicing. Using this NDI method a number of LAU7A guide rails were considered to be cracked beyond a length acceptable for service and the technique has since been used to monitor crack growth in launcher guide rails.

An alternative inspection technique, also utilising eddy current technology has been used by AESF. This technique has not always given the same result as that given by the method used at 481 Wing. One reason for the differences in the results is that the method of detection used at 481 (a moving coil galvanometer) is not as sensitive to changes in signal as an oscilloscope and hence, small ridges developed under the guide rail often produce spurious results [2], which has led to the rejection of some rails which cannot be shown to be cracked by this alternative NDI technique.

To enable a simpler detection of crack growth AMRL developed an NDI method which utilised ultrasonic techniques. This method did not require the removal of the missile from the launcher guide rail and so was used for most of the LAU-7/A fatigue testing program. The crack-length results obtained by this method were compared with results obtained by the eddy current method developed by AESF. Some of the data are summarised in Table B1.1.

The general lack of agreement between the two techniques is somewhat disappointing and attests to the difficulty in making such measurements. It is not possible to assess the accuracy of the two methods used here without breaking open the guide rails and checking against actual crack lengths.

B2. Summary of AMRL Ultrasonic Method, [3]

B2.1 Equipment:

Krautkramer USIP12 or similar
 5MHz, 60 Degree shear wave probe (Automation Industries Type 2MZ)
 Test Piece, NDISL/EC146

Medium Viscosity Couplant (Automation Industries)

B2.2 Set-up Procedure:

Gain 60 dB
Range 50
Frequency 5 (narrow band)
Filter 3
Reject 2.5
Position IP at 0 on the Time Base

B2.3 Method of Operation

1. Connect the probe to the flaw detector and position it on the test piece away from the artificial defect, as shown in Figure B2.1.
2. Move the probe toward and away from the outboard corner and observe the return signals; the signal from the outboard corner may be identified by tapping the outboard corner and noting the attenuation of the return signal as shown in Figure B2.2.

Note that the return signals may vary considerably depending on the physical size of the 60° probe used and therefore little guidance can be given as to exactly what signal shape and position to expect. The figures in this appendix should be regarded as guides only. Great care should be taken to be sure that the probe is positioned to give maximum response from the outer corner.

3. When the optimum response is obtained from the outer corner mark the position of the probe on the test piece and then mark this position with a line parallel to the outboard edge.
4. Move the probe along this line, maintaining the maximum return signal from the outboard corner. When the probe is opposite the artificial defect, a signal will appear between the IP and the return from the outboard corner, Figure B2.3. Maximise this signal by small adjustments to the probe position on the side of the rail, then carefully mark the position of the probe on the test piece.
5. Once a satisfactory position has been achieved, locate the return from the artificial defect and position the alarm gate (if available) to activate the alarm.
6. Inspect launcher guide rails using steps [1] to [5], above.
7. To simplify "in-service" inspections, it is recommended that the probe be cast into a shoe which locates it relative to the outboard edge of the rail as shown in Figure B2.4. It is suggested that "PlastiBond" filler/casting material be used to cast the shoe whilst the probe is clamped into position on the test piece such that it gives maximum response from the artificial defect.
8. When the probe/shoe assembly is completed, re-position the shoe on the test piece and slide it along the outboard edge, making sure that the response from the artificial defect is similar to that seen prior to the casting of the shoe. If this is not the case, the shoe must be re-cast.

9. LAU-7/A launcher guide rails can then be inspected, without disassembly of the system. During the testing program covered by this report it was found that a minor modification of the shoe would permit the inspection of the rails, without the removal of the missile.

B3. References

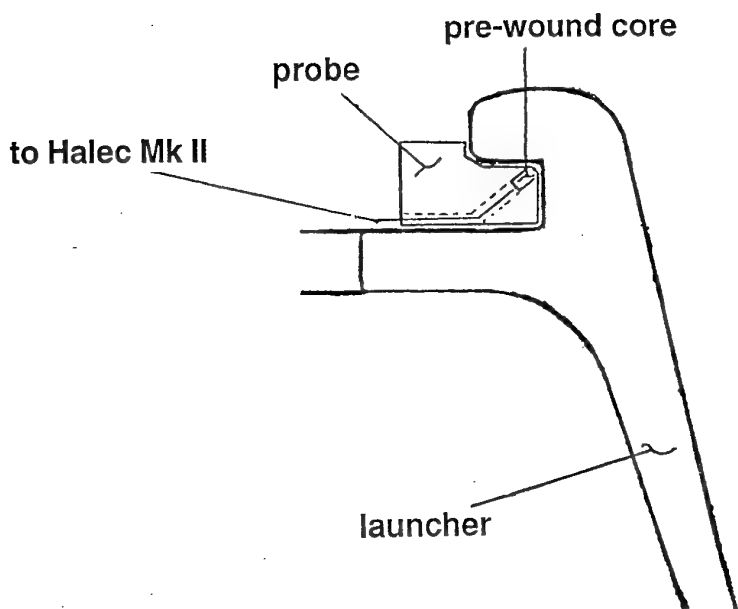
1. RAAF NDISL "LAU-7/A Launcher - Non Destructive Inspection Procedure" STI - Armament Airborne Equipment / 196.
2. Kirk, D. "LAU-7/A Launcher Non-destructive Inspection Procedure Report." RAAF internal report, May 1989.
3. Bishop, B and Morton, H. "Ultrasonic Inspection of LAU-7/A Launcher Guide Rail." DSTO Aeronautical Research Laboratory, Aircraft Materials Division, Technical Memorandum 502, December 1989.

Table B1.1. Crack length measurements on LAU-7/A launcher guide rails

LAUNCHER SERIAL NUMBER	EDDY CURRENT		ULTRA SONIC	
	left (mm)	right (mm)	left (mm)	right (mm)
188	-	44	-	27
268	22.5	-	-	
377	35	-	24	-
396	14	26	51	-
442	29.5	37	-	-
714	-	(1)	5	*
757	27	-	35	29
773	35	-	50	20
816	-	32	-	-
1351	-	16.5	-	-

Note:

1. Rail removed, no recorded NDI measurement.



*Figure B2.1 The original Eddy Current technique as used by the RAAF.
(from [1] AESF)*

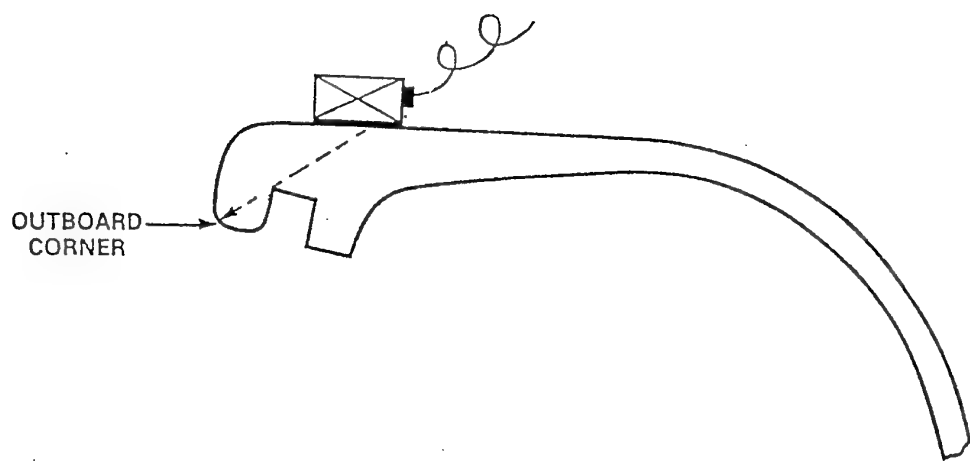


Figure B2.2 The outboard corner reflection measured by a correctly positioned ultrasonic probe. This new technique was developed at AMRL [3]

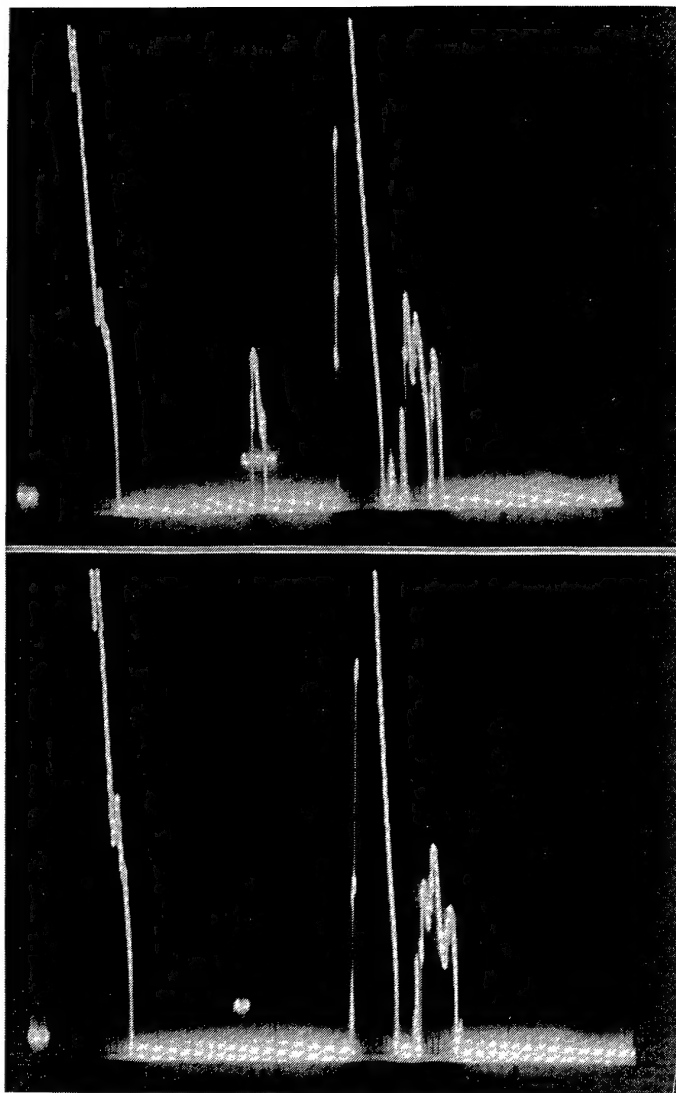


Figure B2.3 The reflection from crack (or artificial defect), within the gate, and outboard corner reflection.

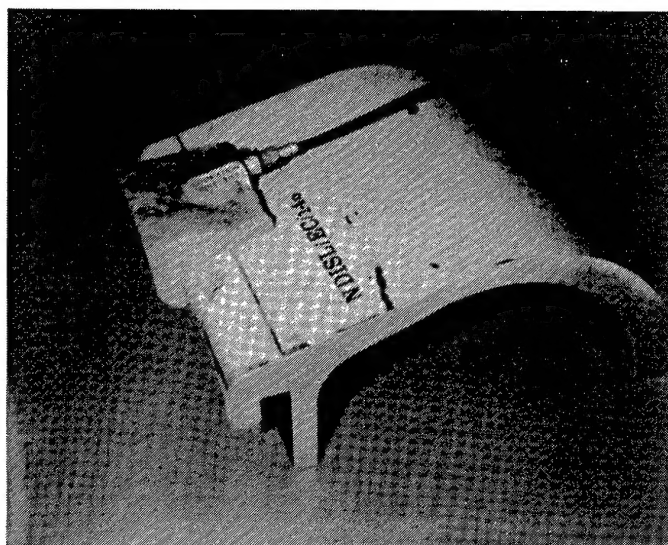


Figure B2.4 Cast shoe for correct positioning of the probe.

Investigation of Fatigue Cracking on LAU-7/A Launcher Housing

D.S. Saunders, M.G. Stimson, R. Bailey and E. Kowal

DSTO-TR-0229

DISTRIBUTION

AUSTRALIA

DEFENCE ORGANISATION.

Defence Science and Technology Organisation

Chief Defence Scientist	} shared copy
FAS, Science Policy	
AS, Science Corporate Management	
Counsellor, Defence Science (London) (Doc Data Sheet only)	
Counsellor, Defence Science (Washington)	
Scientific Adviser to Thailand MRD (Doc Data Sheet only)	
Scientific Adviser to the DRC (Kuala Lumpur) (Doc Data Sheet only)	
Senior Defence Scientific Adviser/Scientific Adviser Policy and Command (shared copy)	
Navy Scientific Adviser (Doc Data Sheet only)	
Scientific Adviser - Army (Doc Data Sheet only)	
Air Force Scientific Adviser (Doc Data Sheet only)	
Director Trials	

Aeronautical and Maritime Research Laboratory

Director
Chief, Airframes and Engines Division
Chief, Ship Structures and Materials Division
J.G. Sparrow
D. Graham (IFOSTP) 3 copies
G. Clark

Authors:

D.S. Saunders (SSMD)
M.G. Stimson
R. Bailey
E. Kowal

DSTO Library

Library Fishermens Bend
Library Maribyrnong
Main Library DSTOS (2 copies)
Library, MOD, Pyrmont (Doc Data Sheet only)

Defence Central

OIC TRS, Defence Central Library
Officer in Charge, Document Exchange Centre (12 Copies)
Defence Intelligence Organisation
Library, Defence Signals Directorate (Doc Data Sheet only)

Air Force

Aircraft Research and Development Unit
Tech Reports, CO Engineering Squadron, ARDU
Director General Policy and Plans
Director Air Warfare
AHQ CSPT
HQ Logistics Command

CLSA-LC
WEAPENG2A
WEAPENG2B

Army

Director General Force Development (Land) (Doc Data Sheet only)
ABC4 Office, G-1-34, Russell Offices, Canberra (4 copies)
Army Technology and Engineering Agency

Navy

Aircraft Maintenance and Flight Trials Unit
RAN Tactical School, Library
Director Naval Engineering Requirements - Aviation Systems
Director Aircraft System Engineering - Navy
Director of Naval Air Warfare
Superintendent, Aircraft Maintenance and Repair
Director Naval Architecture
ASSTASS, APW2-1-OA2, Anzac Park West, Canberra (Doc Data Sheet only)

UNIVERSITIES AND COLLEGES

Australian Defence Force Academy
Library
Head of Aerospace and Mechanical Engineering
Deakin University, Serials Section (M list)), Deakin University Library, Geelong, 3217,
Senior Librarian, Hargrave Library, Monash University

OTHER ORGANISATIONS

NASA (Canberra)
AGPS

ABSTRACTING AND INFORMATION ORGANISATIONS

INSPEC: Acquisitions Section Institution of Electrical Engineers
Library, Chemical Abstracts Reference Service
Engineering Societies Library, US
American Society for Metals
Documents Librarian, The Center for Research Libraries, US

INFORMATION EXCHANGE AGREEMENT PARTNERS

Acquisitions Unit, Science Reference and Information Service, UK
Library - Exchange Desk, National Institute of Standards and Technology, US
National Aerospace Laboratory, Japan
National Aerospace Laboratory, Netherlands

SPARES: 11 copies

TOTAL 80 copies

DEFENCE SCIENCE AND TECHNOLOGY ORGANISATION DOCUMENT CONTROL DATA		1. PRIVACY MARKING/CAVEAT (OF DOCUMENT)	
2. TITLE Investigation of Fatigue Cracking on LAU-7/A Launcher Housing		3. SECURITY CLASSIFICATION (FOR UNCLASSIFIED REPORTS THAT ARE LIMITED RELEASE USE (L) NEXT TO DOCUMENT CLASSIFICATION) Document (U) Title (U) Abstract (U)	
4. AUTHOR(S) D.S. Saunders, M.G. Stimson, R. Bailey and E. Kowal		5. CORPORATE AUTHOR Aeronautical and Maritime Research Laboratory PO Box 4331 Melbourne Vic 3001	
6a. DSTO NUMBER DSTO-TR-0229		6b. AR NUMBER AR-008-405	
8. FILE NUMBER M1/8/788		9. TASK NUMBER AIR 88/053	
10. TASK SPONSOR WEAPENG 2		11. NO. OF PAGES 69	
13. DOWNGRADING/DELIMITING INSTRUCTIONS		14. RELEASE AUTHORITY Chief, Airframes and Engines Division	
15. SECONDARY RELEASE STATEMENT OF THIS DOCUMENT <i>Approved for public release</i> OVERSEAS ENQUIRIES OUTSIDE STATED LIMITATIONS SHOULD BE REFERRED THROUGH DOCUMENT EXCHANGE CENTRE, DIS NETWORK OFFICE, DEPT OF DEFENCE, CAMPBELL PARK OFFICES, CANBERRA ACT 2600			
16. DELIBERATE ANNOUNCEMENT No limitations			
17. CASUAL ANNOUNCEMENT Yes			
18. DEFTEST DESCRIPTORS F/A-18 aircraft Missile Launchers Cracking (fracturing)			
19. ABSTRACT <p>A number of LAU-7/A launcher housings on Australian F/A-18 aircraft have been found to be fatigue cracked at the location of the forward missile hanging bracket. This was initially ascribed to poor aft snubbing of the missile in the launcher guide rail.</p> <p>An investigation of the response of the LAU-7/A launcher housing configuration to static and fatigue loading was undertaken to determine the failure mechanism.</p> <p>A test fixture was designed to apply static loads to a launcher housing via a dummy AIM-9 missile. The results showed that the strains at the points of engagement of the missile hanging brackets with the launcher guide rail were not significantly influenced by the effectiveness of the aft snubbing of the missile.</p> <p>The launcher housing was then fatigue tested using spectrum loading. The loads applied to the test articles were derived from a number of N_z load spectra of Australian F/A-18 aircraft. The load levels were factored up to account for the dynamic effects of the flexible wings of the aircraft. To ascertain whether the loads achieved in the experimental study were appropriate for the fatigue testing of the component, the fracture surfaces derived from the fatigue test were compared with several surfaces removed from launcher housings which had failed under operational loads. The results showed that the use of "factored" N_z loads was only an approximate simulation of the wing tip environment, but in the absence of a wing tip spectrum these loads gave approximately similar fatigue fracture surfaces to those of the components in service.</p> <p>The results showed that the cracking was largely induced by the inertial loads experienced by the missile, which are transferred to the guide rails of the LAU-7/A housing.</p>			